Alison Jacqueline Pestana Setim

Licenciada em Ciências da Engenharia Química e Bioquímica

Upgrade of an Experimental Volumetric Unit for Gas Adsorption Equilibrium Studies

Dissertação para obtenção do Grau de Mestre em
Engenharia Química e Bioquímica

Orientador: Isabel A. A. C. Esteves, Investigadora Auxiliar, FCT/UNL

Co-Orientadores: José P. B. Mota, Professor Catedrático FCT/UNL

Rui P. P. L. Ribeiro, Investigador Pós-Doutoramento, FCT/UNL

Presidente: Professor Doutor Mário Eusébio
Arguente: Doutora Inês do Nascimento Matos
Vogal: Doutor Rui P. P. L. Ribeiro

FACULDADE DE CIÊNCIAS E TECNOLOGIA
UNIVERSIDADE NOVA DE LISBOA

Setembro 2014

Alison Jacqueline Pestana Setim

Licenciada em Ciências da Engenharia Química e Bioquímica

Upgrade of an Experimental Volumetric Unit for Gas Adsorption Equilibrium Studies

Dissertação para obtenção do Grau de Mestre em
Engenharia Química e Bioquímica

Orientador: Isabel Esteves, Investigadora Auxiliar, FCT/UNL

Co-Orientadores: José P. B. Mota, Professor Catedrático FCT/UNL

Rui P. P. L. Ribeiro, Investigador Pós-Doutoramento, FCT/UNL

Presidente: Professor Doutor Mário Eusébio
Arguente: Doutora Inês do Nascimento Matos
Vogal: Doutor Rui P. P. L. Ribeiro

FACULDADE DE CIÊNCIAS E TECNOLOGIA
UNIVERSIDADE NOVA DE LISBOA

Setembro 2014

É com enorme orgulho e gratificação que dedico esta tese aos meus pais, Maria Setim e João Sardinha e, a uma pessoa muito especial que, embora ausente, me irá guiar para sempre, João Setim.

Agradecimentos

A elaboração desta tese de mestrado não seria possível sem o esforço contínuo na sua construção mas também sem a colaboração e ajuda que recebi. Desta forma gostaria de agradecer, em primeiro lugar, aos meus orientadores, Doutora Isabel Esteves e Doutor Rui Ribeiro, que se disponibilizaram para me orientar durante a tese de mestrado. Pelo profissionalismo, pelos conhecimentos transmitidos, colaboração, preocupação, paciência e disponibilidade para ajudar.

Agradeço a todas as pessoas do grupo de investigação pela forma como fui recebida, pela atenção e disponibilidade. Em especial ao Professor Doutor Paulo Mota, pelo exemplo de competência científica e a Bárbara Camacho pela disponibilidade, apoio e paciência que demonstrou ao longo destes seis meses.

Gostaria também de agradecer à Faculdade de Ciências e Tecnologias – Universidade Nova de Lisboa pelas condições de trabalho que ao longo destes anos proporcionou, possibilitando a concretização de este Mestrado.

Um agradecimento muito especial à Ana Cristina Dias pela enorme amizade, carinho, confiança e incondicional apoio que sempre demonstrou.

Gostaria também de agradecer o apoio incondicional prestado pelo Alexandre Faria que me deu forças para não desistir desta enorme jornada e por estar sempre presente em todos os momentos constituindo uma parte muito especial dos meus dias. Obrigado pelas palavras de força, coragem e confiança transmitidas que foram sem dúvida acolhedoras e de grande valor nesta minha caminhada.

Não podia deixar de agradecer à minha família, principalmente aos meus pais e irmão que nunca me deixaram desamparada incentivando-me sempre a cumprir este meu objectivo. Agradeço aos três pelo apoio, pela ajuda, paciência, incentivo e pelo exemplo de vida que guiou a pessoa que sou hoje.

Abstract

In this work, a volumetric unit previously assembled by the research group was upgraded. This unit revamping was necessary due to the malfunction of the solenoid valves employed in the original experimental setup, which were not sealing the gas properly leading to erroneous adsorption equilibrium measurements. Therefore, the solenoid valves were substituted by manual ball valves.

After the volumetric unit improvement its operation was validated. For this purpose, the adsorption equilibrium of carbon dioxide (CO_2) at 323K and 0 - 20 bar was measured on two different activated carbon samples, in the of extrudates (ANG6) and of a honeycomb monolith (ACHM). The adsorption equilibrium results were compared with data previously measured by the research group, using a high-pressure microbalance from Rubotherm GmbH (Germany) – gravimetric. The results obtained using both apparatuses are coincident thus validating the good operation of the volumetric unit upgraded in this work.

Furthermore, the adsorption equilibrium of CO_2 at 303K and 0 - 10 bar on Metal-Organic Frameworks (MOFs) Cu-BTC and Fe-BTC was also studied. The CO_2 adsorption equilibrium results for both MOFs were compared with the literature results showing good agreement, which confirms the good quality of the experimental results obtained in the new volumetric unit. Cu-BTC sample showed significantly higher CO_2 adsorption capacity when compared with the Fe-BTC sample.

The revamping of the volumetric unit included a new valve configuration in order to allow testing an alternative method for the measurement of adsorption equilibrium. This new method was employed to measure the adsorption equilibrium of CO_2 on ANG6 and ACHM at 303, 323 and 353K within 0-10 bar. The good quality of the obtained experimental data was testified by comparison with data previously obtained by the research group in a gravimetric apparatus.

Keywords: Equilibrium Adsorption; Adsorption Isotherms; Adsorbent Materials; Adsorbates; Volumetric Method

Resumo

Neste trabalho a unidade volumétrica previamente desenhada e construída pelo grupo de investigação foi modificada. Esta alteração foi necessária devido a problemas de operação válvulas automáticas utilizadas na unidade original, visto que as mesmas não garantiam o completo controlo do gás levando a problemas na determinação de dados de equilíbrio de adsorção. Desta forma, as válvulas automáticas foram substituídas por válvulas de bola de operação manual.

Após a alteração da unidade volumétrica, o seu foi validado. Para tal, o equilíbrio de adsorção de dióxido de carbono (CO_2) a 323K e 0 -10 bar foi medido em duas amostras de carvão activado, na forma de extrudados (ANG6) e monólito tipo favo-de-mel (ACHM). Os dados de equilíbrio de adsorção obtidos foram comparados com dados previamente obtidos pelo grupo de investigação utilizando uma microbalança de alta precisão para medição a alta pressão da Rubotherm GmbH (Alemanha) – método gravimétrico. Os resultados obtidos utilizando as duas instalações são coincidentes, validando o bom funcionamento da unidade volumétrica alterada neste trabalho.

Adicionalmente, o equilíbrio de adsorção de CO_2 a 303K e 0 - 10 bar em dois metal-organic frameworks, Cu-BTC e Fe-BTC foi também estudado. Os resultados de equilíbrio de adsorção de CO_2 em ambos os MOFs foram comparados com os dados de literatura mostrando boa coincidência, o que confirma a boa qualidade dos resultados experimentais obtidos na nova instalação volumétrica. A amostra de Cu-BTC mostrou uma capacidade significativamente mais alta para adsorção de CO_2 do que a amostra de Fe-BTC.

A alteração da unidade volumétrica incluiu uma modificação da configuração de válvulas, de modo a permitir testar um método alternativo para a medição de equilíbrios de adsorção. Este novo método foi utilizado na medição do equilíbrio de adsorção de CO_2 em ANG6 e ACHM a 303, 323 e 353K entre 0 - 10 bar. A boa qualidade dos resultados experimentais foi confirmada por comparação com dados obtidos pelo grupo na instalação gravimétrica.

Palavras-Chave: Equilíbrio de Adsorção; Isotérmicas de Adsorção; Materiais Adsorventes; Adsorbatos; Método Volumétrico

List of Contents

List of Figures

List of Tables

Chapter I

1. Introduction

1.1. Motivation

With the rapid increasing of the global population and industrialization, the consumption of energy from combustion of fossil fuels is dramatically growing. The current dependence on fossil fuels, as a primary source of energy, relies to the inherent energy density, abundance, and also on economic factors [1, 2]. Even though, the fossil fuels play an important role in power generation and industrial manufacturing, their combustion releases a large amount of CO_2 into the contributing to the greenhouse effect [2]. The CO_2 concentration in the atmosphere, nowadays, is close to 400 ppm which is significantly higher than the pre-industrial level of about 300 ppm [3].

The primary sources of anthropogenic greenhouse gas emissions, like CO_2, are referenced by the *Inventory of U.S Greenhouse Gas Emissions and Sinks*. Electricity production (32%), transportation (28%) and industry (20%) are the sectors that most contribute to the emissions of carbon dioxide to the atmosphere [4].

In addition to the efforts to reduce energy consumption and develop renewable energy sources, CO_2 capture and storage (CSS) emerge as an option. Therefore, important research work on efficient technologies to capture CO_2 has been done recently [5, 6]. According to the *Intergovernmental Panel on Climate Change (IPCC)* [1], the emissions of CO_2 to the atmosphere can be reduced by approximately 80-90% for a modern power plant that is equipped with suitable carbon dioxide capture and storage (CCS) technologies.

CO_2 capture can be performed in three different routes: pre-combustion, oxyfuel and post-combustion [7]. Post-combustion CO_2 capture involves a gas separation process of the industrial combustion effluents. Various technologies have been studied for this application including physical absorption, chemical absorption, and membranes and also, adsorption processes [8]. There are many studies of CO_2 separation and storage using solid adsorption processes and a variety of solid adsorbent have been proposed due to their properties including surface area, pore volume, pore size distribution, regeneration procedure and cost. The extensive list of studied adsorbents for CO_2 capture includes zeolites [9], activated carbons [10] and more recently, metal organic frameworks (MOFs) [2] [11]. The knowledge of CO_2 adsorption equilibrium and the chosen adsorbent is of paramount importance for the design of an efficient adsorption-based separation processes for CCS, such as Pressure Swing Adsorption (PSA) and Temperature Swing Adsorption (TSA) [12,13].

In this work, an in-house developed volumetric unit for the measurement of adsorption equilibrium was upgraded. The new experimental unit was validated by measuring the adsorption equilibrium of CO_2 on two different carbon-based adsorbents and two MOFs between 303 and 373K and 0 - 10 bar. The obtained results experimental data was compared with the results previously obtained by the

research group in high-precision gravimetric unit, to testify its good quality. Furthermore, a new alternative method for volumetric adsorption equilibrium measurements was tested and the obtained results confirmed the feasibility of the new procedure.

1.2. Structure of the Thesis

Besides this introductory chapter, this thesis is structured with the following contents:

- **Chapter II:** Background

In this chapter the theoretical fundamentals regarding the adsorption phenomena are discussed and the latest developments that have been made in this research field are reviewed. A brief description of the adsorbents, activated carbons and metal-organic frameworks, studied in this thesis is also presented.

- **Chapter III:** Volumetric Unit Upgrade, Calibration and Validation

This chapter presents the experimental procedure for the volumetric unit previously built by the research group, as well as the experimental test results obtained. The upgrade of the volumetric unit is also described with detail. The experimental adsorption equilibrium measurements results of CO_2 on ANG6 and ACHM activated carbon samples obtained using the upgraded apparatus are also presented. These results were successfully compared with gravimetrically obtained data, validating the good functioning of the unit. Adsorption equilibrium of CO_2 over Cu-BTC and Fe-BTC was also measured and is reported in this chapter.

- **Chapter IV:** Alternative Volumetric Method for Adsorption Equilibrium Determination

In this chapter, an alternative method for the measurement of adsorption equilibrium using the revamped volumetric apparatus is explained and the experimental procedure is described. The experimentally obtained results for the adsorption equilibrium measurement of CO_2 on ANG6 carbon and ACHM at 303, 323 and 353K and 0 - 10 bar are reported. A comparison between the volumetric and gravimetric experimental data results is also presented.

- **Chapter V:** Conclusions and Future Work

In this chapter the main conclusions and suggestions for future work are summarized.

Chapter II

2. Background

In this chapter the main concepts regarding the adsorption phenomena, including adsorption equilibrium isotherms theory, are discussed. The theoretical background of the traditional experimental method employed in this work is discussed, and an alternative method is presented. Finally, the fundamentals of the adsorbent materials tested within this work are also presented.

2.1. Adsorption Phenomena

Adsorption is an exothermic phenomenon and it corresponds to the enrichment of one or more of the components of a fluid phase in the interface region with a solid surface [14]. This phenomenon is different from absorption, in which the species diffuse into a liquid or solid and is, therefore, taken up by volume; in contrast, adsorption is a surface phenomenon [15]. In adsorption processes, porous solids are commonly employed as adsorbents to ensure a large superficial area and microporous volume which allow good adsorption capacities [16].

Adsorbate molecules accumulate onto the surface of the adsorbent until its adsorption capacity is achieved and the equilibrium at the thermodynamic conditions under study is reached. Adsorption applications range many industrial levels for gas separation, storage or purification processes, characterization of porous materials, and others [14, 15].

Depending on how the adsorbed molecules interact with the solid two phenomena can be distinguished: chemisorption and physisorption. In physisorption the adsorbate-adsorbent interactions are weaker than the chemical bonds which characterize chemisorption. Therefore, when dealing with physisorption the adsorbates can generally be released (desorbed) by increasing the temperature or reducing the partial pressure of the adsorbates in the gas phase [17]. On the other hand, in chemisorption sorbent regeneration is more energy intensive and frequently cannot occur without changing the adsorbent properties [18].

When the adsorption phenomena starts, the adsorbent material possesses a large number of active sites, and the number of molecules adhering to the adsorbent surface (i.e. being adsorbed) exceeds the number of molecules leaving the surface (i.e. being desorbed) [15]. As the surface becomes covered with the adsorbates, the probability of an adsorbate molecule to find an available site decreases. The equilibrium state is reached when the rate of adsorption equals the rate of desorption [19]. The amount of gas retained by the adsorbent, after reaching the equilibrium, defines the adsorption capacity of the adsorbent towards a specific adsorbate.

Adsorption processes science is a field of increasing interest for innumerous industrial applications. Adsorption-based processes are widely used for separation of gas mixtures [20], hydrogen purification [21, 22], capture and separation of carbon dioxide mostly resultant from the

combustion of fossil fuels [23], biogas upgrading [24, 25], capture and recovery of volatile organic compounds (VOC's) [26] and others.

Cycle engineering is of the great importance in the development of continuous adsorption-based separation processes, but the adsorbent properties and its interaction with the adsorbed species are also of great importance. For this purpose, it is extremely important to study the adsorption equilibrium data of the adsorbates over the adsorbent materials involved in a specific process. The adsorption equilibria data is normally presented as **adsorption isotherms** which give the relation, at constant temperature, between the amount adsorbed and the equilibrium pressure, or concentration. Although adsorption isotherms are the most commonly type of graphical presentation of equilibrium data there are others options like **isobars**, which present the amount adsorbed by temperature at constant pressure, and **isosteres** which relate the equilibrium pressure with temperature for a constant amount adsorbed [27].

2.2. Adsorption Equilibrium: Isotherms

Adsorption isotherms describe the amount of adsorbate retained on the adsorbent surface as a function of pressure (if gas) or concentration, at constant temperature, and also give information about the characteristics of the adsorbent employed. The adsorption isotherm describes the equilibrium between the fluid-phase concentration and the concentration in the adsorbent particles, at a given temperature. The quantity adsorbed is commonly normalized by the mass of the adsorbent to allow comparison between different materials [14] [28].

Adsorption isotherms are related with the pore size of the adsorbent since the porosity can limit the adsorption capacity of the material and influence the shape of the isotherm. Adsorption isotherms may be used to characterize porous solids and design industrial adsorption processes. According to IUPAC classification there are six different types of adsorption isotherms. The first five types (I to V) of the classification were originally proposed by Brunauer, Deming, Deming and Teller as the BDDT classification (1940), sometimes referred to as the Brunauer classification (1945) [17]. The different types of isotherms considered in the IUPAC classification are showed in Figure 2.1.

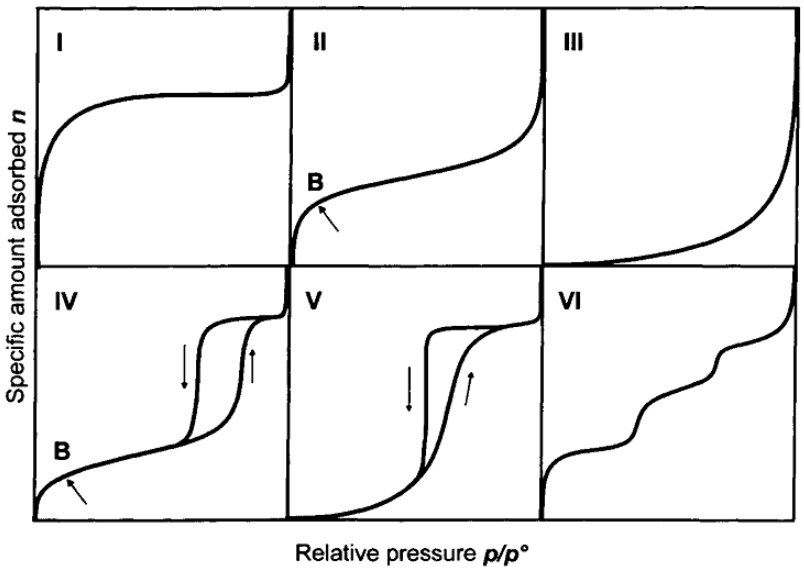

Figure 2.1 - IUPAC classification for adsorption isotherms [9]

Type I isotherms are characteristic for microporous materials. The interactions between the solid surface and the gas molecules result in an increase in adsorption, especially at low pressures. These isotherms, also known as Langmuir Type isotherms, are thus characterized by a plateau that is almost parallel to the pressure axis [17] [27].

Type II isotherms typically describe adsorption in mesoporous adsorbents, non-porous surfaces and some compacted powders. This type of isotherms occurs due to monolayer adsorption at low pressures followed by multilayer adsorption, at higher pressures. The point B (in Figure 2.1 II) represents the starting point of multilayer adsorption and the ending of the monolayer section. These isotherms can be described by the BET equation or its generalizations [15] [17].

Type III isotherms are very uncommon and are characterized by their convex behavior relatively to the pressure axis. This feature is indicative of weak adsorbent – adsorbate interactions. [14]

Type IV isotherms are similar to type II isotherms and are characteristics of monolayer – multilayer adsorption as well. In this case the main difference is the presence of hysteresis which is associated with capillary condensation taking place in mesopores [17] [27].

Type V isotherms are given by mesoporous and microporous solids and very similar to type III. They both present a convex behavior along the axis of relative pressure but the relevant difference between them is the occurrence of two inflection points and hysteresis [17].

Type VI isotherms are also rare and are associated with layer to layer adsorption on a highly uniform non-porous surface. The sharpness of the steps is conditioned by the system and temperature. The height of each step is related to the adsorption capacity of each layer [14] [17].

This classification must be viewed as a simplification since many experimental isotherms have a hybrid nature and their degree of complexity is variable. Moreover this type of isotherm classification only applies to the adsorption of a single component gas within its condensable range of temperature [14].

2.3. Adsorbent Materials: General Concepts

Adsorbents are porous solid materials with a high surface area capable of adsorbing molecules from liquids or gases, and may be classified according to their pores average diameter [29]. The classification of pore size according to IUPAC is often used to characterize the material [16] as shown in Table 2.1.:

Table 2.1 – IUPAC pore size classification [16]:

Adsorbent Characterization	
Microporous adsorbents	d < 2 nm
Mesoporous adsorbents	2 < d < 50 nm
Macroporous adsorbents	d > 50 nm

The adsorbent material plays an important role in adsorption processes since the effectiveness of both equilibrium and kinetics of adsorption are dependent on the properties of the solid and the adsorbate species.

The selection of an efficient adsorbent for a specific application must consider the adsorption equilibrium and kinetics properties of all constituents in the gas mixture, within the pressure and temperature range of operation. Considering a binary mixture, its separation can be promoted due to different adsorption capacity of the adsorbent towards each species (equilibrium separation) or, on the other hand, due to significant differences in the kinetics of each component (kinetic separation) [16].

An effective adsorbent is the one that is easily regenerated and present the perfect combination between adsorption capacity and kinetics [30]. In order to meet these requirements, the following aspects must be taken into account [16]:

a) The solid must have reasonably large surface area and/or a considerable micropore volume;
b) The solid must have relatively large pore network for the transport of molecules to the micropores.

Although there are many adsorbents to choose from, the research and development of enhanced adsorbents can improve the performance of current adsorption processes. The development of such adsorbents is also important to extend the use of adsorption processes to other applications.

The most commonly used adsorbents in industry are the **activated carbons** due to their large micropore and mesopore volume, high surface area (BET-area can be larger than 2000 m^2/g) [14] and the variety of functional groups on its surface. Their particular surface properties make the activated carbons suitable adsorbents for many processes [30-34].

Activated carbons are produced starting with the original pores present in the raw material and more porosity, with desired size distributions, is created by the activation process which can be by two different methods: gas and chemical [30].

Activated carbons have the advantage of being available at low prices and being produced in several morphologies (beds, pellets, monoliths, fibers and others) [30], [35], [36]. In this work, the adsorption equilibrium of CO_2, between 303 -373K and 0 – 10 bar, on two activated carbons, including pelletized carbon and a honeycomb monolith was studied.

There are also other important adsorbents like silica gel, zeolites and more recent metal organic frameworks (MOFs). **Silica Gel** has the appearance of a hard glassy substance, is milky white in color and it is made from the coagulation of a colloidal solution of silicic acid [30]. This adsorbent is used in most industries because of its desiccant properties being useful in water removal processes [37, 38] and gas drying [39]. Depending on the synthesis procedure silica gel can have a surface area between 200 m^2/g and 900 m^2/g [16].

Zeolites are crystalline aluminosilicates of alkali or alkali-earth elements, such as sodium, potassium and calcium. Like activated carbons, zeolites are commonly used as adsorbents. These materials occur naturally or be synthetized in many types (A, X, Y, modernite, ZSM, etc.) [16]. The major use of zeolites is in petrochemical cracking, ion exchange (water softening and purification), and in the separation and removal of gases and solvents [30].

More recently a new class of materials, **metal organic frameworks (MOFs)**, also known as porous coordination materials, has been gaining importance. MOFs are highly crystalline inorganic-organic materials that are formed by assembling metal-containing clusters known as building units with multidentate organic ligands (such as carboxylates, tetrazolates, sulfonates) by coordination bonds [40, 41]. Due to their chemical and thermal stability, permanent porosity and high surface area, MOFs are considered adsorbents of great potential in the chemical industry namely for H_2 storage applications [40], CO_2 capture [42], drug delivery [41], catalytic processes [43] and other applications.

The functionalization of the organic component of the framework, or the incorporation of functional organic groups directly into the framework, may yield porous solids that contain different groups enhancing its more selectivity [42]. The increasing interest on more efficient adsorbents has motivated the synthesis of more MOF structures and, consequently, this has become a field of interest for research and development purposes [44].

In this work, the adsorption equilibrium of CO_2 at 303-373K and 0-10 bar over three MOF samples, MIL-53(Al), Cu-BTC and Fe-BTC was studied.

a) MIL-53(Al) MOF

The MIL-53(Al), or Aluminium Terephthalate, is a hydrophilic MOF that can be used for adsorption applications. This is a very interesting class of MOFs because they not only adsorb large quantities of gas, but also presents an exceptional flexibility undergoing a reversible structural transformation between two distinct conformations – large pore (lp) and narrow pore (np). Both conformations share the same chemical composition. At room temperature and in the absence of the

adsorbate molecules, the lp phase is the most stable form. However, during gas adsorption, the lp phase becomes np at low pressures and inverse transformations occurs at higher pressures [45 - 47].

b) Cu-BTC MOF

Cu-BTC is one of the most studied MOFs for gas adsorption presenting a potential interest for separation of polar and non-polar species [48]. Cu-BTC [Cu^3 (BTC), BTC= 1,2,3-benzenetricarboxylate], also known as HKUST-1, is commercially available by the trade mark of Basolite C300^{TM} synthesized by BASF SE (Germany) with a surface area between 1500 and 2100 m^2/g [49]. This MOF, has a unique structure with a Cu based center and corners linked by BTC linkers. This configuration gives the material a multiple pore characteristic and adsorption sites that improve adsorption process [50].

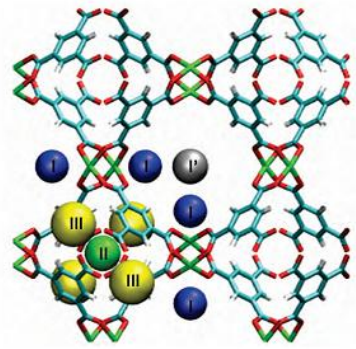

Figure 2.2 - Structure of Cu-BTC metal organic framework [45].

Figure 2.2 the CU-BTC structure is represented showing the BTC molecules forming an octahedral shape in the corners. Each corner contains two copper atoms that are bonded to the oxygen atoms of four BTC linkers forming four-connected square-planar vertexes [51]. The remaining axial coordination sites, usually referred to as open metal sites are stable after exposure to liquid water. This is particularly important to improve adsorption selectivity for separating mixtures with molecules of different polarities especially at low pressures [51, 52]

This MOF has been largely used as an adsorbent for various applications such as biogas upgrading [53], adsorption of organosulfur compounds [54, 55], gas storage, separation and purification [50] [56 – 58] and others.

c) Fe-BTC MOF

Fe-BTC is a new MOF adsorbent with potential interest in chemical, biomedical and biochemical industries [59]. This iron based MOF is commercially available by the name of Basolite^{TM} F300 synthesized by BASF SE (Germany) with a surface area between 1300 and 1600 m2/g [60].

Although scarce information is available in the literature at this point, the structure of Fe-BTC is expected to be closely related to that of MIL-100. MIL-100 is constructed by trimmers of iron octahedral linked by the BTC moieties in such way that it promotes a mesoporous structure accessible

by microporous windows [59]. Even though the reported surface area of Fe-BTC is smaller than MIL-100 one, the specific area of Fe-BTC is still larger and it is reasonable to assume that Fe-BTC should display most of the characteristics features of MIL-100 [61]. Unlike MIL-100(Fe) there are not many studies of Fe-BTC as an adsorbent material published in the actual literature [62 – 64].

2.4. Adsorption Equilibrium Measurement: Experimental Methods

Adsorption equilibrium of gaseous compounds can be measured employing different methods. In this section, the two most widely used methods (gravimetric and volumetric) are described.

2.4.1. Gravimetric Method

The gravimetric method is a method which evaluates the adsorption equilibrium of gases in porous solids by mass weighting. This is a relatively simple method in which a certain amount of gas is brought into contact with an adsorbent sample while the pressure, temperature and mass increase of the sample are monitored and recorded. Although the principle is quite simple, the design and construction of a gravimetric apparatus is not straightforward. The adsorbent containing vessel is usually a conventional metal system, but the balance must have a very high-precision [65].

Figure 2.3 shows a simple gravimetric experimental setup. The experimental procedure usually starts by placing a sample of the adsorbent material in the adsorption vessel followed by the sample activation which can be performed by evacuation, heating and flushing with helium [15] [66]. Helium is used for this purpose because it can be considered a non-adsorptive gas at atmospheric pressure and room temperature [15], [67].

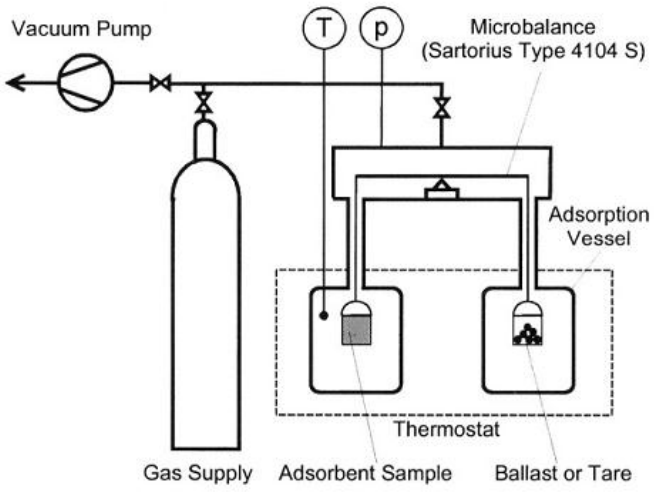

Figure 2.3 - Experimental setup for gravimetric measurements of pure gas adsorption equilibria [15]

After the adsorbent activation and initial mass measurement, the adsorptive species are introduced into the adsorption vessel up to the desired pressure; equilibrium is thus reached when the

mass and the pressure measurements remain constant at the temperature of the experiment [68]. This method presents the advantage of being significantly more accurate than the volumetric method.

2.4.2. Volumetric / Manometric Method

The volumetric method, also known as manometric method, is the oldest technique used in the measurement of gas-phase adsorption equilibrium. This method consists in an indirect measurement of the amount adsorbed and despite being less precise than gravimetric method it can give accurate results when using suitable equipment and procedures [66].

A volumetric adsorption equilibrium experiment consists in feeding an amount of adsorptive gas into a calibrated volume. Then, the gas stored in the calibrated volume is expanded into a cell containing the previously activated (as in the gravimetric method) adsorbent material. Adsorption takes place and a fraction of the gas is adsorbed on the adsorbent surface, while another fraction remains in the gas-phase. The amount of adsorbed gas can then be calculated by a mass balance considering the gas-phase before and after adsorption. For this procedure, both volumes (calibrated and adsorbent cell volumes) must be previously known [66] [15].

The volumetric method is an efficient technique for measurement of adsorption equilibrium isotherms. This method presents the advantages of being easier to implement and less expensive than the gravimetric method. On the other hand, the significant disadvantage of the method are the experimental errors caused by indirect determination of the adsorbed amount of gas [66], and the consecutive expansions of the adsorptive which is reflected in the accumulation of even more experimental errors. In contrast, the gravimetric method errors are not cumulative and are only dependent of the measuring equipment. In order to obtain the desired adsorption equilibrium isotherm, the procedure has to be repeated as many times as the amount of points desired since each assay to only one point of the isotherm. Table 2.2 summarizes the principal advantages and disadvantages of the volumetric method employed in the measurement of adsorption equilibria.

Table 2.2 - Advantages and disadvantages of the volumetric method used to measure adsorption equilibria data [10]

Volumetric Method: Advantages and Disadvantages	
Advantages	• It is simple, easy to implement and do not require complex and expensive technology. • It relies on the accuracy of the pressure and temperature measurements (considering that, the mass of the adsorbent sample used is known and the apparatus volumes have been previously determined).

Disadvantages	• Traditionally, in volumetric adsorption equilibrium measurements adsorbent degassing is not performed between each isotherm point determined. For this reason, the experimental error is cumulative for each point (i.e. the error of the previously measured point must be taken into account in the forthcoming point. • The determination of the amount of gas adsorbed is an indirect measurement according to a mass balance deduced and it can lead to a bigger uncertainty.

In this work, the described traditional volumetric method for the determination of adsorption equilibrium data is employed. Furthermore, an alternative method for adsorption equilibrium measurements with the volumetric unit is presented. This method is similar do the one described but instead of measuring adsorption equilibria at constant temperature, the gas amount inside the adsorption chamber is maintained constant and the temperature is changed. The experimental procedure will be explained with detail in Chapter 4.

The principal advantage of this non-conventional method is that enables the user to measure three adsorption isotherms by varying the temperature. Also, there is no need for adsorbent re-activation of the samples between isotherms introducing less experimental error.

2.5. Summary

In this chapter the theoretical fundamentals regarding the adsorption phenomena were discussed and the latest developments that have been made in this research field are reviewed. A brief description of the adsorbents, activated carbons and metal-organic frameworks, studied in this thesis is also presented.

The interest in the knowledge of the properties of pure gases is strictly linked to the objective of performing their purification and separation from different gas streams. The knowledge of CO_2 adsorption equilibrium, in particular, and the chosen adsorbent is of paramount importance for the design of an efficient adsorption-based separation processes for CCS, such as Pressure Swing Adsorption (PSA) and Temperature Swing Adsorption (TSA) [12, 13].

Chapter III

3. Volumetric Unit: Upgrade, Calibration and Validation

A recent home-made volumetric unit was the starting point of this thesis [69]. The work that was recently developed with this apparatus revealed several drawbacks. Therefore, an upgrading of the existing volumetric equipment, its subsequent calibration and experimental validation were required and are presented in this work.

The original volumetric unit was employed to study the adsorption equilibrium of ethane over two adsorbents: an activated carbon, ANGUARD 5 (ANG5) and the metal organic framework MIL-53(Al), both materials previously studied and characterized by the group [45][70 – 73]. During these adsorption studies it was confirmed that the solenoid valves used in the original volumetric unit could not properly seal the gas in the desired section within all the pressure range employed in the experimental procedure.

Due to the confirmation of this valve malfunction, changes in the volumetric unit had to be performed. During this re-arrangement the experimental unit was also upgraded in order to allow testing an alternative method for the measurement of adsorption equilibria. This method is described in detail, in Chapter 4.

In this chapter the results obtained in the previously built unit regarding the adsorption equilibrium of ethane in the MIL-53(Al) and ANG5 at 303, 323 and 373K within 0-20bar are presented and compared with data previously measured by the research group, using a high-pressure microbalance from Rubotherm GmbH (Germany) – gravimetric method.

After the volumetric unit improvement its operation was validated. For this purpose, the adsorption equilibrium of carbon dioxide (CO_2) at 323K and 0 - 20 bar were measured on two different activated carbon samples, in the of extrudates (ANG6) and of a honeycomb monolith (ACHM) and the results were compared with data previously measured by gravimetry in our group. Furthermore, the adsorption equilibrium of CO_2 at 303K and 0 - 10 bar on Metal-Organic Frameworks (MOFs) Cu-BTC and Fe-BTC was also studied.

3.1. Experimental

3.1.1. Apparatus Description

The original experimental apparatus was designed to allow the simultaneous measurement of adsorption equilibrium on two adsorbent samples up to 20bar over a wide temperature range (303-1373K) [69]. The assembled apparatus was built with stainless steel tubing (Swagelok Company, USA), and nine solenoid valves (ASCO Numatics., USA) that were controlled by an home-made control and data acquisition software developed in Labview environment. Two

pressure transducers (Omega Eng. Inc., USA) measure the operation pressure in the range of 0 to 20 bar with an uncertainty of 0.05% of the Full Scale (FS); The apparatus includes two stainless steel (SS) vessels (Swagelok, USA) of 40 cm^3 of volume each, used to obtain a certain reference volume (V_{ref}); Two Pt-100 probes (RS Amidata, Spain), placed inside of each reference volume, measuring the temperature of that unit section, while an oven (Nabertherm B170 GmbH, Germany) with a temperature range of 303K to 1373K enclosed the two sample cells at a constant temperature. Figure 3.1 and 3.2 presents the general view of the original volumetric unit, and a schematic of the volumetric unit originally built [69], respectively. The auxiliary volume is a known volume used only for calibration.

Figure 3.1 - General view of the original volumetric unit

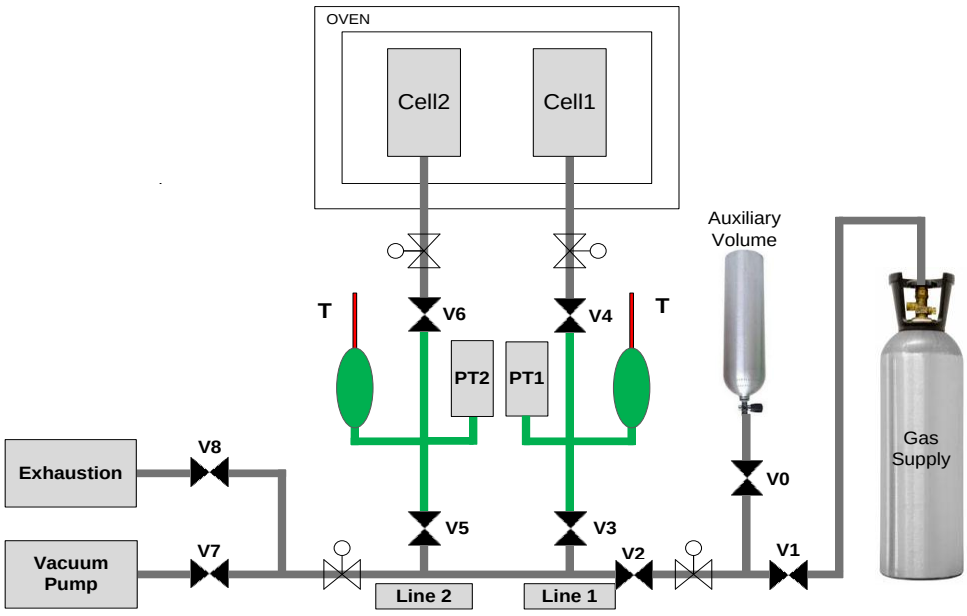

Figure 3.2 – Schematic representation of the original volumetric unit. The green section represents the reference volume (Vref); PT denote the pressure transducers and V denote the valves and T the Pt100 sensors.

The adsorption equilibrium measurements using the volumetric unit follow a standard procedure [15] [30] [74, 75]. The calibration of the reference and cell volumes of the original volumetric unit was previously done by the research group [69].

Prior to adsorption measurements it is important to ensure the absence of leaks. For this purpose helium is fed into the unit and pressure variations are monitored. Helium is generally used for this method considering the assumption that it does not adsorb at low pressure and ambient temperature [15] [67]. In these conditions if the pressure drops, the presence of leaks must be considered and repaired. After ensuring the absence of leaks in the system, the gas is fed into the reference volume presented in Figure 3.2 (green section) by opening the valves V1, V2, V3 and V5 with V4, V6, V7 and V8 closed.

To begin the adsorption equilibrium measurements, the adsorbent has to be activated (degassed) in order to remove impurities and moisture. The activation of the samples at a known temperature depends on the adsorbent characteristics. In this case, the adsorbents were activated *in situ* by heating the samples at 373.15K for the ANG5 and 473K for the MIL-53(Al) under vacuum conditions (for 3 to 4 hours) before each experiment. The heating-rate of the oven is set to 2 K/min until the required temperature for activation is reached. The slow temperature increase reduces the temperature impact in the sample structure and prevents any damages.

In order to measure an adsorption isotherm, the gas fed into the reference volume is expanded into the sample cell while the pressure is measured by the two pressure transducers PT1 and PT2. As adsorption takes place the pressure decreases until the equilibrium is established, this is assumed to occur when the pressure becomes constant and origins a plateau.

The equilibrium state generally takes a few hours to be established depending on the characteristics of the adsorbent-adsorbate system under study. When the equilibrium is established the valves V4 and V6 are closed and the procedure is repeated as many times as desired taking into account the limit range of the pressure transducers which is 20 bar.

The desorption equilibrium measurements are done in similar way as the adsorption ones, but instead of feeding the gas into the reference volume it has to be released using the exhaustion stream line. This way, when the maximum pressure is reached, a similar procedure is repeated, but this time by stepwise depressurization of the reference volume and subsequent contact with the adsorption cells. This checks possible hysteresis effects [76].

3.1.2. Materials

Regarding the materials used as adsorbents, the metal organic framework MIL-53(Al) synthesized by the BASF SE (Germany) under the trademark Basolite A100 was used in the form of powder with an average pore diameter of *32 µm,* according to the manufacturer [69] [73]. This material is largely studied because of it flexibility and adsorption capacity, being able to adsorb large amounts of gas like H_2, CO_2 and light alkane [45] [77]. On the other hand, the

ANG5 carbon supplied by *Sutcliffe Speakman Carbons Ltd. (UK*) is a pelletized carbon (2 mm diameter extruded) with high density and activity [70]. The activated carbon extruded form is an interesting morphology for gas separation process applications since it allows decreasing the adsorption bed pressure drop, has good mechanical strength and less dusting when compared with powdered materials, which are unpractical for industrial applications [70].

Approximately 0.3 grams of each material were employed in the experimental measurements, after a proper activation *in situ*, under vacuum at 373K for the activated carbon and 473K for the MOF. All gases used in the work were supplied *Air Liquide (Portugal*): CO_2 N48, C_2H_6 N35 and He N50.

3.2. Theory

Adsorption equilibrium data are often reported as excess amount adsorbed (q_{ex}) which gives the amount of gas adsorbed in excess that occupies the same volume at the same pressure and temperature, if the gas is not adsorbable in the solid [31]. The mass balance employed in the determination of the excess amount adsorbed is presented in Equation (1):

$$q_{ex} = \frac{1}{m_s}\left[V_{ref}\left(\rho_{ref.i} - \rho_{ref.f}\right) + (V_c - V_s)\left(\rho_{cell.i} - \rho_{cell.f}\right) + q_{ex-1}\right] \qquad \textbf{Equation (1)}$$

where m_s correspond to the solid mass activated, V_{ref} is the reference volume, Vc and Vs are the cell volume and the solid volume respectively and $q_{ads\text{-}1}$ is the amount of gas adsorbed in the previous step, ρ_{ref} and ρ_{cell} are the densities of the bulk gas in the reference volume and in the cell at the initial pressure (i) and temperature and after expansion at pressure and temperature of equilibrium (f). This density values were obtained using the *NIST* database [78].

The total amount adsorbed (q_t) is related to the excess amount adsorbed by the equation 2 where V_p is referred to the pore volume of the adsorbent and ρ_g is the density of the gas [79]. This quantity considers the adsorbed phase as well as the coexisting gas within the pore volume of the adsorbent [70]:

$$q_t = q_{ex} + V_p\rho_g \qquad \textbf{Equation (2)}$$

Gumma and Talu [79] have recently proposed a new thermodynamic quantity, net amount adsorbed (qnet), to report adsorption equilibrium data. It is the total amount of gas present in the measuring cell with the adsorbent minus the amount that would be present in the empty cell (without the adsorbent) at the same pressure and temperature. This quantity can be related to q_{ex} by Equation (3) where *Vs* is the solid volume [73]:

$$q_{ex} = q_{net} + V_s\rho_g \qquad \textbf{Equation (3)}$$

The advantage of reporting adsorption results in therms of qnet is that it completely circumvents the use of probe molecules to fix the reference state of each sample since the value of V_{ref} and V_{cell} are independent of the fluid-adsorbent system [73] [79].

3.3. Experimental Results and Discussion

The experimental adsorption equilibrium isotherms of ethane on ANG5 and MIL-53(Al) at 303K, 323K and 373K are presented in Figures 3.3 and 3.4, respectively and the tables listing the obtained results are presented in Appendix A and B. As expected, the isotherms show a decreasing adsorption capacity as the temperature increases since adsorption is an exothermic phenomenon. Despite this fact, in some points the isotherms present an unexpected shape as it is possible to observe in Figure 3.3 for the adsorption equilibrium isotherm of ethane on ANG5 at 373K. The same is observed for MIL-53(Al) where the isotherms for different temperatures intersect each other (Figure 3.4). These observations confirmed that the solenoid valves were not able to work properly within all the experimental conditions. These valves could not work in a bidirectional system, allowing the gas to backflow when pressure variations occurred.

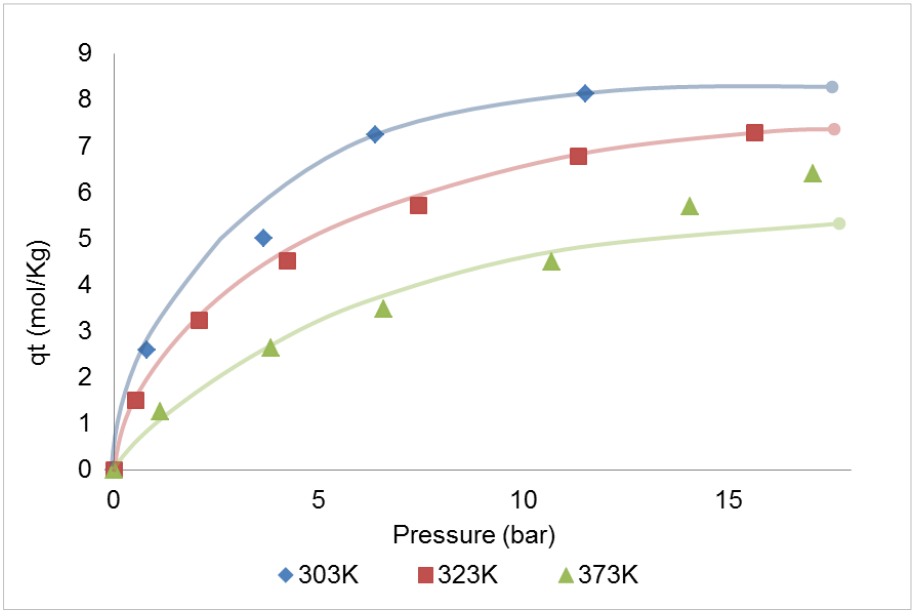

Figure 3.3 – Single-component adsorption equilibrium isotherms for ethane at 303K, 323K and 373K on ANG5. Solid lines are a guide-to-the-eye.

In volumetric adsorption equilibrium measurements, the difference between the initial and final pressure readings, give the amount of gas adsorbed. If there is gas leaving the calibrated volumes without being adsorbed due to the inefficient valve performance, it leads to the determination of erroneous adsorption capacity values. This may be assumed to be the reason

for obtaining experimental results in which the isotherms at different temperatures intercept each other.

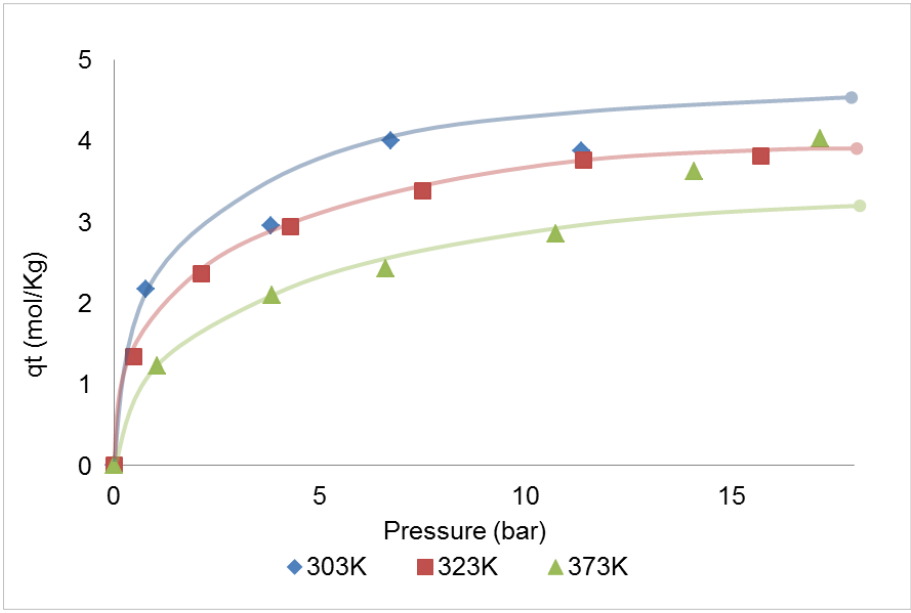

Figure 3.4 - Single-component adsorption equilibrium isotherms for ethane at 303K, 323K and 373K on MIL-53(Al). Solid lines are a guide-to-the-eye.

Compared with ANG5 adsorption results, MIL-53(Al) is most clearly affected by the leaks caused by the solenoid valves. Despite this fact, the isotherm obtained for 323K is in accordance with data previously obtained by the research group using a gravimetric unit, as showed in Figure 3.5 [73]. However, the isotherm obtained at 303K in this work shows dispersed results and could not reproduced satisfactorily the gravimetric data available.

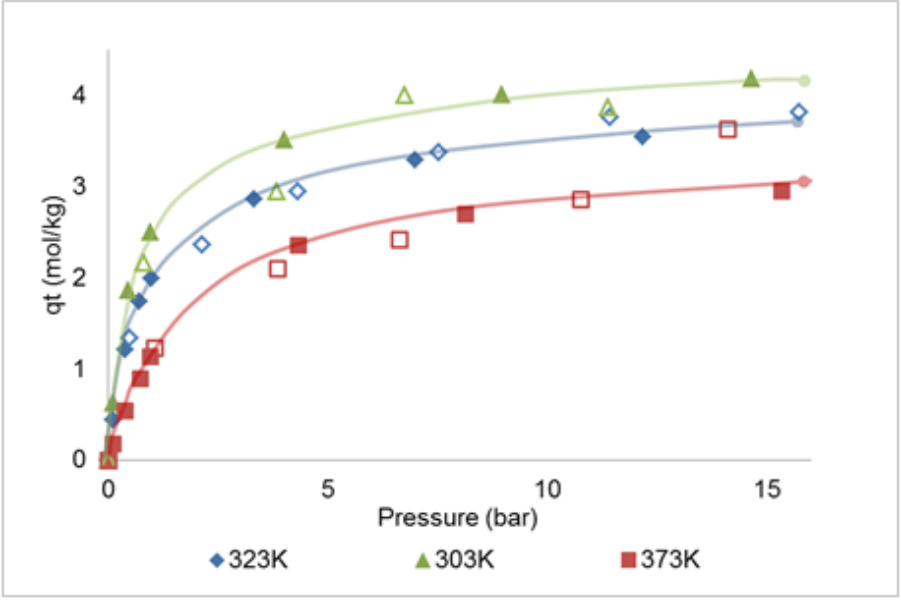

Figure 3.5 - Single-component adsorption equilibrium isotherms for ethane at 303K, 323K and 373K on MIL-53(Al). Filled plots denote the experimental data obtained previously by Gravimetry by the research group [73]; empty plots denote the volumetric results obtained in this work. Solid lines are a guide-to-the-eye.

After 10 bar, the adsorption isotherm measured at 373K was expected to maintain an absolute amount adsorbed lower than 3 mol/kg instead of a total adsorption almost coincident to the one measurement at 323K which indicates a leak of gas.

Subsequently to the analysis of these results it was concluded that the volumetric unit had to be upgraded to allow its correct operation. Therefore, the solenoid valves were substituted by manual ball valves. Furthermore, an additional change in the apparatus was promoted in order to allow testing a new method for the measurement of adsorption equilibrium, as described in Chapter 4.

3.4. Volumetric Unit Upgrade

The upgrading of the unit consisted mainly in the substitution of the solenoid valves for manually operated ball valves. Unlike the automatic solenoid valves, the newly employed ball valves have a spherical disk that permits the total blockage of the gas flow independently of the direction of the flow.

Another important modification to the volumetric unit was performed in order to allow employing an alternative method for adsorption equilibrium measurement. This method consists in maintaining constant the amount of gas inside the adsorption cell and varying the temperature. To perform this new method a new valve configuration had to be designed so that the reference volume could be isolated from the adsorption cell while maintaining the pressure transducer monitoring the pressure inside the adsorption cell. This alteration had to be

performed since the reference volume, which was kept at ambient temperature, has nearly 40 cm^3 while the adsorbent cell volume is inferior to 3 cm^3. Therefore, if the previous unit configuration was maintained it would be unfeasible to test the alternative method proposed in this work, and detailed in Chapter 4. The result of the modifications made to the upgraded volumetric unit is presented in Figure 3.6 and 3.7 and a schematic is showed in Figure 3.8.

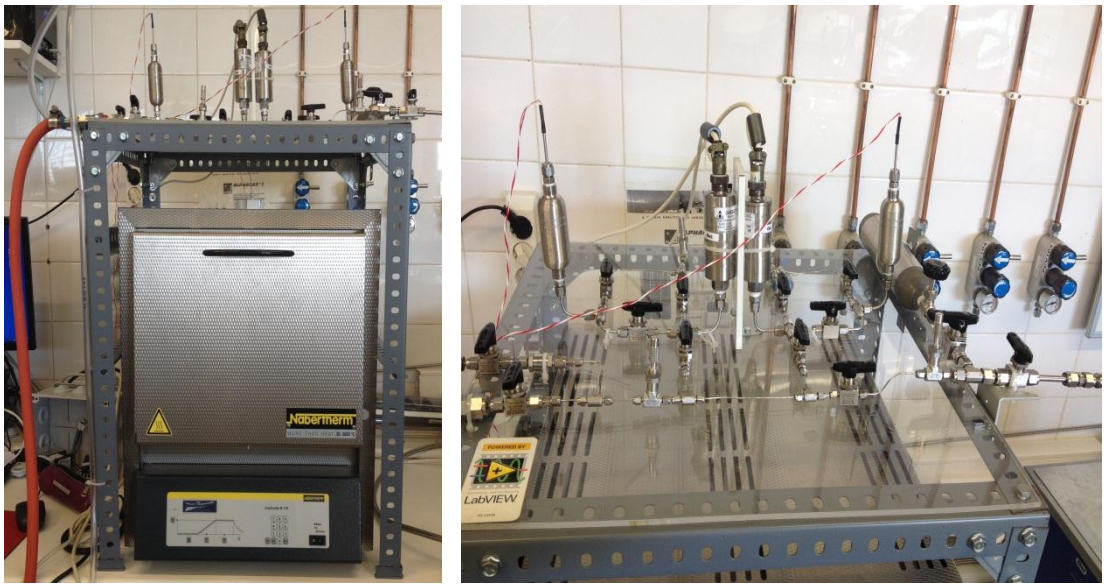

Figure 3.6 - General view of the upgraded volumetric unit

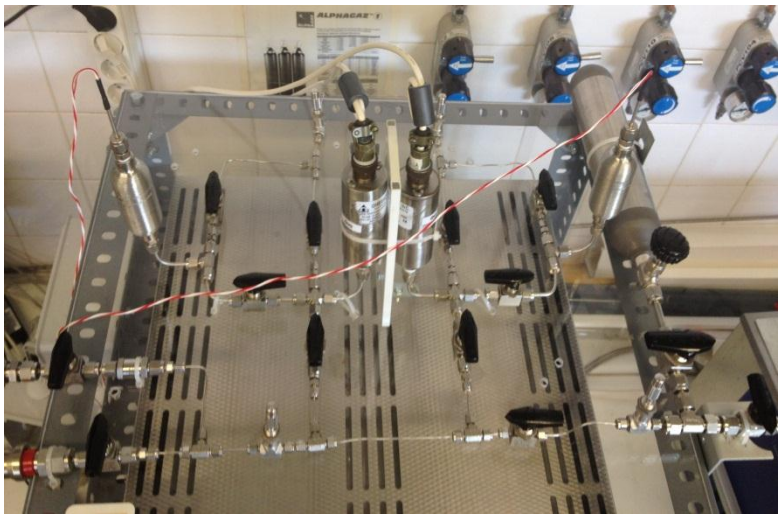

Figure 3.7 - Detail of the volumetric unit main section

Despite the modification of the volumetric unit, the experimental procedure to operate this installation remains similar to the previous one. During the adsorption equilibrium measurements the valve V0 remains closed (Figure 3.8) during the entire process being only used for the reference and cell volumes calibration.

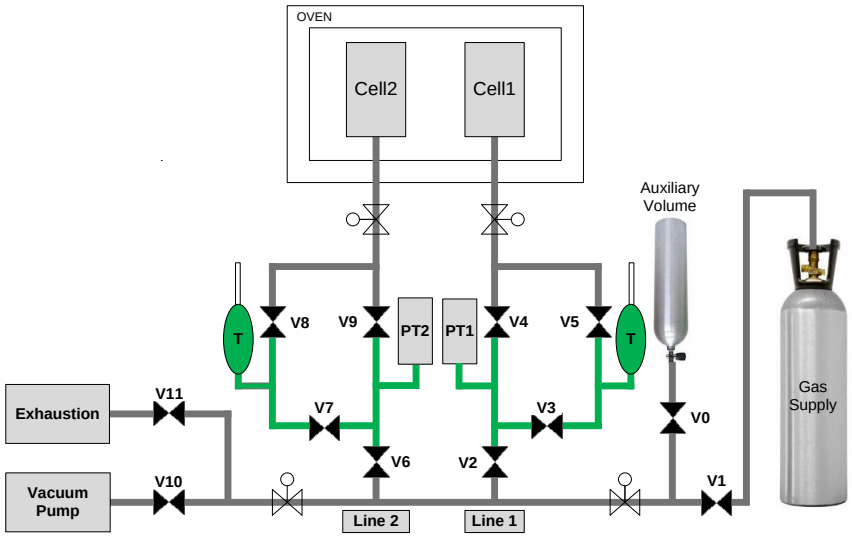

Figure 3.8 - Schematic representation of the upgraded volumetric unit. The green section represents the reference volume (Vref); PT denote the pressure transducers, V the valves, and T the Pt100 sensor.

In the adsorption equilibrium measurements, following the traditional method at constant temperature, the gas is fed into the reference volume represented in green (Figure 3.8) by opening valves V1, V2 and V3, with V4 and V5 closed for line 1, and V6 and V7 open with V8 and V9 closed for line 2. The gas is then enclosed inside the reference volume by closing the valves V2 and V6. After approximately 10 minutes, the gas contained in the reference volume is expanded to the adsorption cells by opening the valves V4, V5, V8 and V9. This way, the adsorbate species contacts with the adsorbent inside the adsorption cells placed in the oven and thus the adsorption occurs. This step is limited by the time needed to reach the equilibrium fluid-solid, after which valves V4, V5, V8 and V9 are closed and the procedure is repeated as many times as necessary but limited to the pressure transducers operation limit, which is 20 bar. When the maximum pressure is reached, depressurization steps to desorb the retained species can be performed by stepwise depressurization of the reference volumes and subsequent contact with the adsorption cells.

3.4.1. Volumetric Unit Upgraded: Reference and Cell Volume Calibration

The modifications of the experimental unit led to different reference and cell volumes that had to be recalibrated. The volumes calibration was performed using a previously determined volume (auxiliary volume in Figure 3.9). The auxiliary volume (334.11cm^3) was calibrated by measuring the weight difference when empty and filled with deionized water (298K) considering the water density of 996.99 Kg/m^3 [80].

Prior to the volumes calibration it is vital to certify that there are no leaks in the unit. After that, the entire experimental unit is evacuated. Then, the auxiliary volume is loaded with gas up

to a pre-defined pressure which is monitored using one of the pressure transducers, as showed in Figure 3.9.

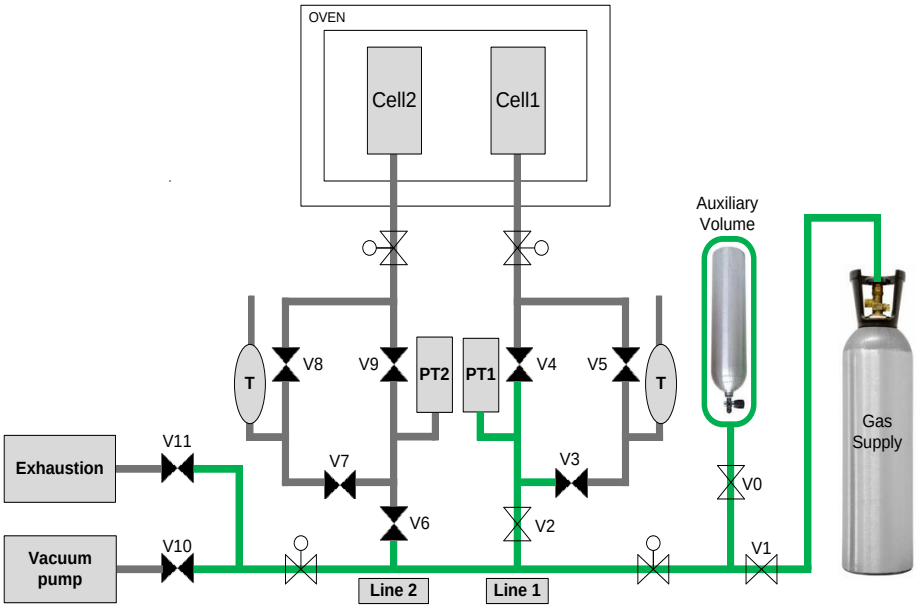

Figure 3.9 - Schematic representation of the first step of the volumes calibration.

After the pressure in the auxiliary volume is registered, the valve V0 is closed and the remaining volume of the experimental unit is depressurized and evacuated, as shown in Figure 3.10. This is performed by opening valve V11 and when atmospheric pressure is reached V11 is closed and V10 is opened to evacuate the system.

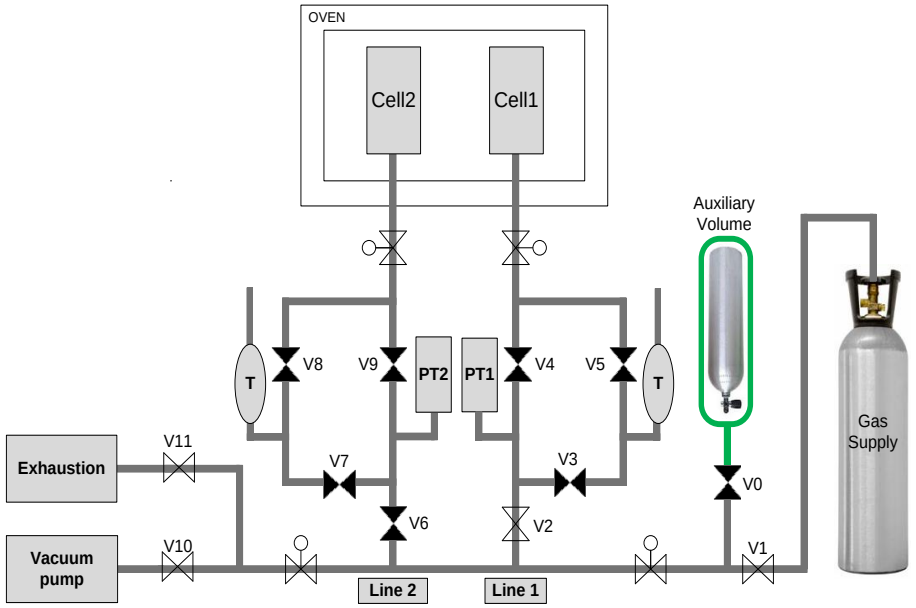

Figure 3.10 - Schematic representation of the second step in the volume calibration.

After the proper degassing of the unit, valves V1, V10 and V11 are closed and the gas in the auxiliary volume is released as shown in Figure 3.11.

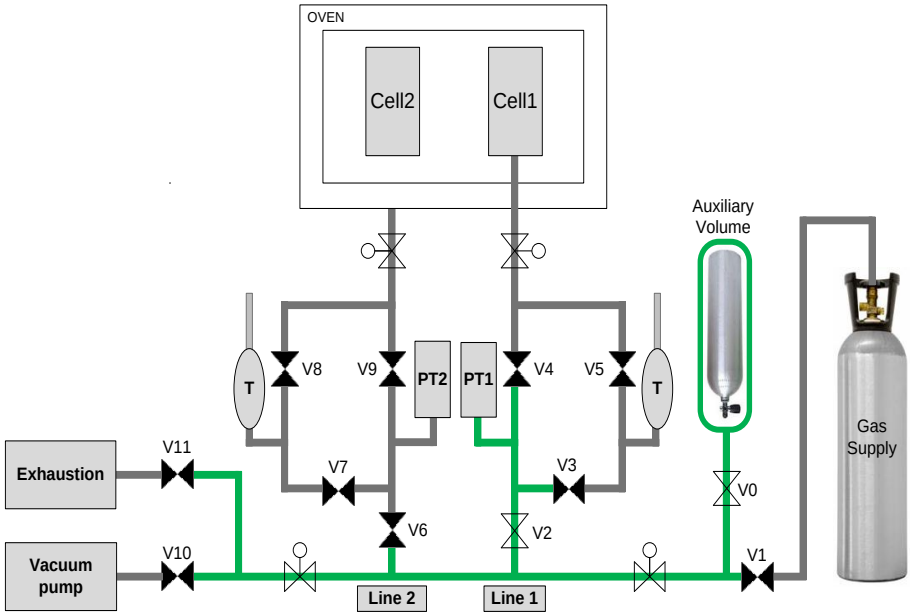

Figure 3.11 - Schematic representation of the third step in the volumes calibration. This step permits the determination of the volume of the green section, V_A.

The pressure is registered in line 1 by opening V2. With this step the volume that comprehends the green line (V_A) represented in Figure 3.11 can be calculated applying the ideal gas law (Equation 5):

$$P\,V = n\,R\,T \qquad \textbf{Equation (4)}$$

Considering that the amount of gas in the experimental unit is maintained constant, the following relation is observed:

$$\frac{P_A \times V_A}{T_A} = \frac{P_{Cylinder} \times V_{Cylinder}}{T_{cylinder}} \qquad \textbf{Equation (6)}$$

where V_A is the green section presented in Figure 3.10 at the temperature T_A and pressure P_A; $V_{cylinder}$ is the auxiliary volume already known at temperature $T_{cylinder}$ and pressure $P_{cylinder}$. As the reference volume and the cylinder are both outside the oven and at room temperature, Equation 6 can be simplified:

$$V_A = \frac{P_{Cylinder} \times V_{Cylinder}}{P_A} \qquad \textbf{Equation (7)}$$

After determination of the volume of the green section, V_A, the valve V6 is opened, as shown in Figure 3.12.

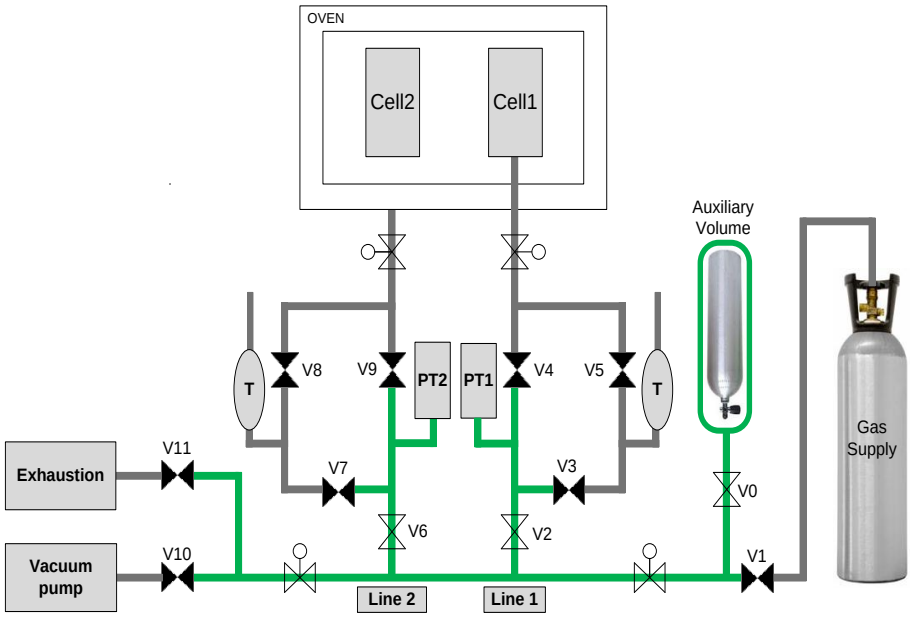

Figure 3.12 - Schematic representation of the fourth step of the volume calibration. This step permits the determination of the volume of the green section, V_B.

As the volume of the section represented in Figure 3.11 is known, the volume (V_B) comprehended by the valves V6, V7 and V9 is calculated by difference, using the pressure registered after this first expansion and following the same logic:

$$\frac{P_B \times V_B}{T_B} = \frac{P_A \times V_A}{T_A} \qquad \textbf{Equation (8)}$$

where V_A is the volume calculated in the third step of calibration (Figure 3.11) at a pressure P_A and temperature T_A. This way the total volume (V_B) of the green section presented in Figure 3.12 can be calculated.

$$V_B = \frac{P_A \times V_A}{P_B} \qquad \textbf{Equation (9)}$$

After the volume V_B is calculated, the first reference volume can be determined by difference applying equation (10). This reference volume (V'_{ref}) corresponds to the section comprehended between valves V6, V7 and V9. The remaining volumes are obtained following the same logic.

$$V'_{ref} = V_B - V_A \qquad \textbf{Equation (10)}$$

The following steps are very straightforward and based on successive expansions, as represented in Figures 3.13 and 3.14, where the volumes are calculated by difference between the initial and the final pressure and employing the ideal gas law.

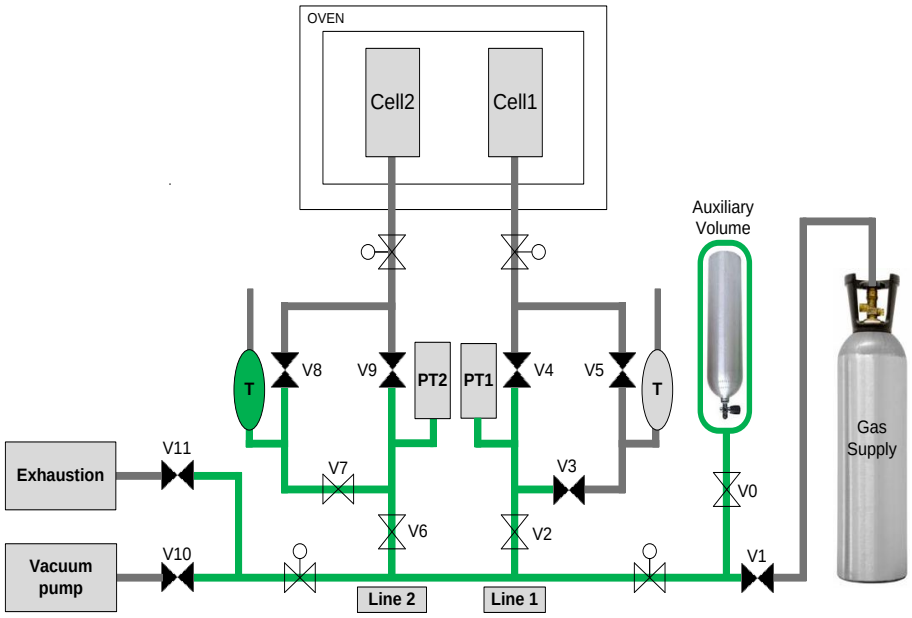

Figure 3.13 - Schematic representation of the fifth step of the volume calibration.

The last step of the volume calibration is the expansion to the adsorption cell (Figure 3.14) which allows the calculation of the cell volume by the same methodology. All the procedure was performed five times in order to minimize the error and obtain averaged values for each volume determined.

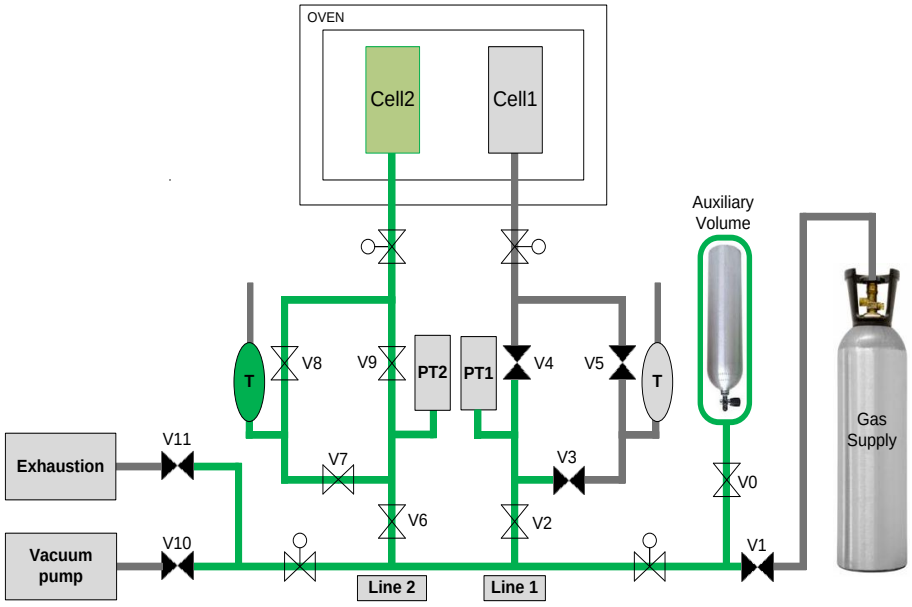

Figure 3.14 - Schematic representation of the sixth step of the volume calibration

In order to calibrate the volumes of line 1, the procedure is repeated symmetrically. The values of the volumes obtained for both lines are showed in Table 3.1:

Table 3.1 – Upgraded volumetric unit calibrated volumes

Results	Line 1	Line 2
V_{cell} (cm^3)	2.03 ± 0.03	1.92 ± 0.03
V_{ref} (cm^3)	41.54 ± 0.03	41.51 ± 0.03
V'_{ref} (cm^3)	2.60 ± 0.01	2.56 ± 0.01

The error of the measurements was determined applying the Standard Combined Uncertainty model (SCU) suggested by the literature [81, 82].

3.5. Validation of the Upgraded Volumetric Unit

The validation of the upgraded volumetric unit was made using both adsorption cells in parallel for the measurement of adsorption equilibrium of CO_2 on two different adsorbents. The experimental results obtained were compared with similar adsorption measurements measured in a high-precision gravimetric unit (Rubotherm GmbH, Germany) [31] [45].

The two adsorbents studied consist in an activated carbon ANGUARD6 (ANG6) presented in the form of extrudates with 1mm diameter, supplied by Sutcliffe Speakman Carbons Ltd. (UK), and an activated carbon honeycomb monolith (ACHM) with cylindrical shape and 20 mm of external diameter, containing 300 cells per square inch. Detailed characterization of the two adsorbents was previously done by the research group [72]. The adsorbate used was carbon dioxide (CO_2, 99.998%) supplied by *Air Liquide Portugal.*

Adsorption equilibrium measurements were performed after both materials were activated *in situ* at 373K (heating rate of 3K/min) under vacuum for a minimum of four hours. Cells 1 and 2 were packed with 0.23g of ANG6 and 0.17g of monolith respectively.

The main properties of the two adsorbents used are presented in Table 3.2. They have approximate surface areas and pore volumes which indicate similar adsorption capacities for both materials.

Table 3.2 - Adsorbents main characteristics [72]

Adsorbents		
	Cell1: ANG6	**Cell2: ACHM**
Pore Volume, V_p (cm^3/g)	0.980	0.990
Solid Density, ρ_s (g/cm^3)	2.62	2.85
Solid Volume, Vs (cm^3)	0.083	0.055

The experimental adsorption equilibrium isotherms of CO_2 on ANG6 and ACHM at 323K are presented in Figures 3.15 and 3.16, respectively. The experimental data (q_t, q_{ex} and q_{net}) is reported in Appendix C and D.

Adsorption equilibrium isotherms of CO_2 on both adsorbents are reported up to 10 bar, despite the fact that the unit was designed to allow measurements up to 20 bar of pressure. This is due to the fact that the adsorption cells employed in the volumetric unit could not avoid gas leaks above 10 bar. This indicates that the adsorption cells must be changed in the future to allow measurements within 0-20 bar.

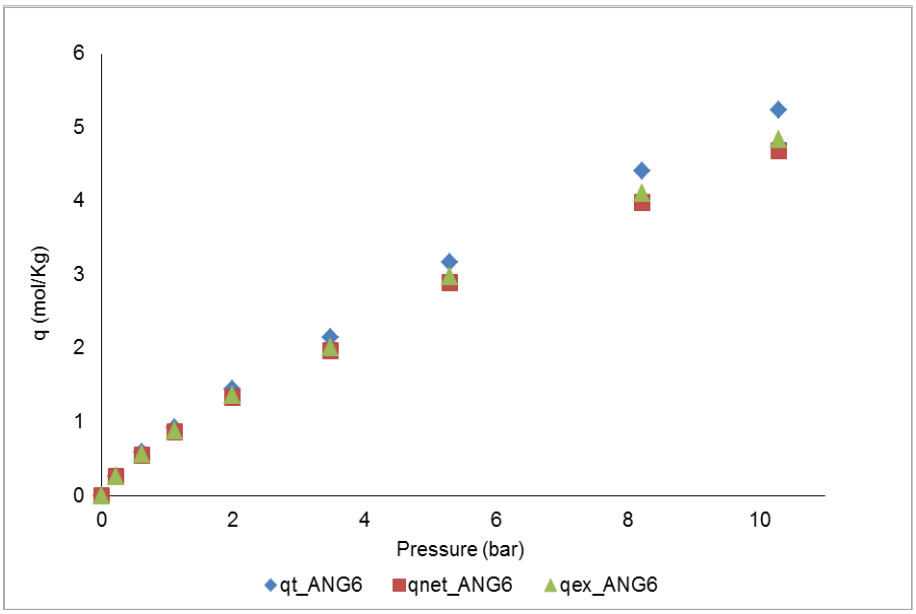

Figure 3.15 – Single-component adsorption equilibrium isotherm for CO_2 at 323K on ANG6.

It is noticed that at low pressures the three amounts (q_{net}, q_{ex} and q_t) are coincident; in contrast as the pressure increases, the difference between the amounts adsorbed for the three quantities become well distinguished which is due to the increasing bulk density. The value for absolute adsorption is always higher than the excess adsorption which is higher than net adsorption, as shown in Figures 3.15 and 3.16.The isotherms describe a Langmuir Type isotherm [74], which is characteristic of microporous materials.

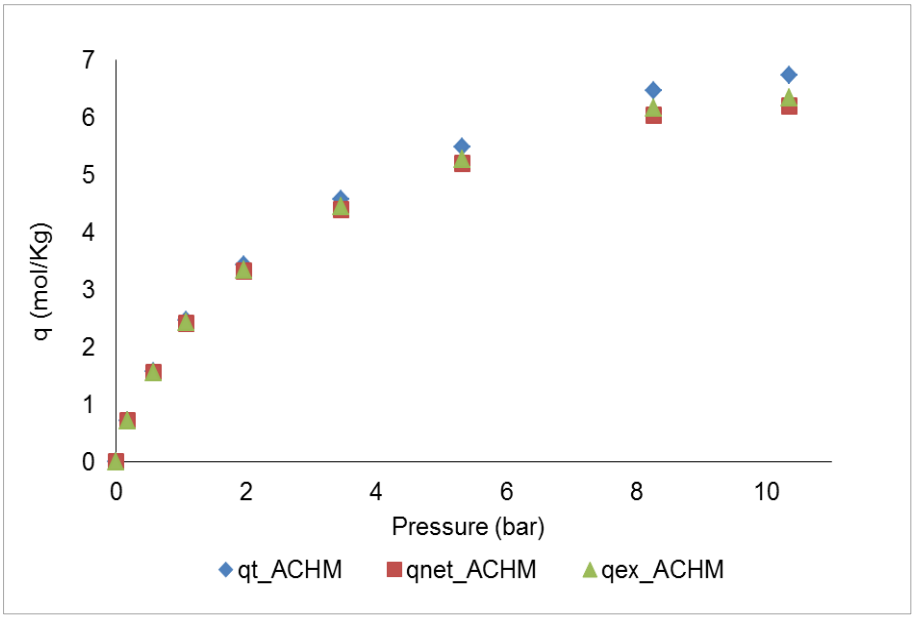

Figure 3.16 - Single-component adsorption equilibrium isotherm for CO_2 at 323K on ACHM monolith.

The results obtained with the modified volumetric unit prove that problem revealed by the previous unit was overcome. The obtained isotherms are perfectly shaped and unlike the previous measurements (with the original volumetric unit), this results shows a great agreement when compared with the results obtained by the high-precision gravimetric unit, performed at the same thermodynamic conditions. Figures 3.17 and 3.18 present the comparison between the CO_2 adsorption equilibrium data at 323K obtained in the gravimetric unit and in the revamped volumetric apparatus in ANG6 and ACHM, respectively.

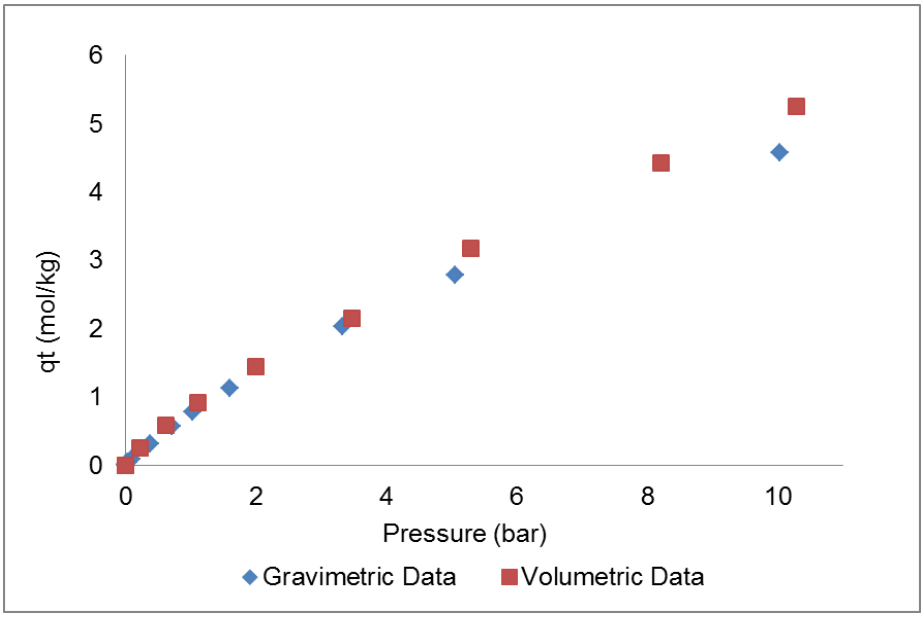

Figure 3.17 - Single-component adsorption equilibrium isotherm for CO_2 at 323K on ANG 6. Comparison between the gravimetric and volumetric data.

The isotherms are coincident for both experimental methods. The difference between the two experimental methods is 7% for the ANG6 and 4% for the ACHM monolith at a pressure value of 6 bar thus validating that the revised volumetric unit is working properly and can be used in future work. It should be noted that at pressures higher than 6 bar the ANG6 present an absolute amount adsorbed higher in the volumetric experiment than in the gravimetric perhaps because of the cumulative error presented by the volumetric method, due to the consecutive gas loading and subsequent expansion.

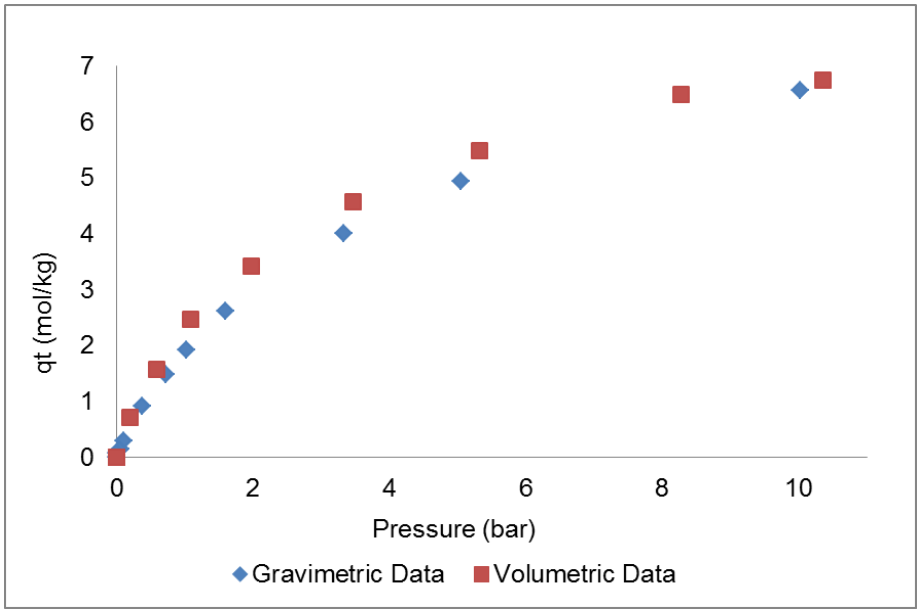

Figure 3.18 - Single-component adsorption equilibrium isotherm for CO_2 at 323K on ACHM monolith. Comparison between the gravimetric and volumetric data.

3.6. Adsorption Equilibrium of CO_2 on Metal-Organic Frameworks Cu-BTC and Fe-BTC

Carbon dioxide adsorption equilibrium measurements at 303K were also carried out on two different powdered MOFs materials, Cu-BTC and Fe-BTC, both synthesized by BASF SE (Germany) under the trade mark of Basolite C300^{TM} and Basolite F300^{TM}, respectively. For these experiments, 0.12g of Fe-BTC were packed in cell 1 and 0.13g of Cu-BTC were placed in cell 2. Prior to measuring the isotherms the samples were activated *in situ* at 473K (temperature increased at a heating rate of 2K per minute), for four hours and under vacuum. The physical properties of the materials are listed in Table 3.3.

Table 3.3 – Physical properties of the adsorbents Cu-BTC and Fe-BTC

Adsorbents		
	Cell1: Fe-BTC	**Cell2: Cu-BTC**
Surface Area, S (m^2/g) [49]	1300-1600	1500-2100
Reactivation Temperature (K) [49]	473	473
Pore Volume, Vp (cm3/g) [83]	0.400	0.610
Solid Density, ρs (g/cm3) [84]	1.677	1.663

The adsorption equilibrium isotherms of CO_2 at 303K in Fe-BTC and Cu-BTC in terms of q_{net}, q_{ex} and q_t, are presented in Figures 3.19 and 3.20 respectively. The experimental data is listed in Appendix E and F. The adsorption equilibrium point obtained at higher pressure (approximately 10 bar), for each adsorbent does not follow the same trend as the lower pressure points. This was due to the adsorption cell malfunctioning which could not avoid gaseous leaks when pressures of around 10 bar or higher are reached. This gas sealing problem observed is due to the fact that the adsorbent containing cell was adapted from a Swagelok filter. This piece was not conceived for sequential opening and closing, reason why after several cycles of opening/closure and heating up to high temperatures, it started to allow CO_2 leaks.

The Fe-BTC adsorbent is a new material that is not well studied reason why there are not many adsorption experimental data available. This makes interesting to study this material for several potential applications. The adsorption equilibrium isotherm obtained for CO_2 over Fe-BTC adsorbent is a Type I isotherm [74]. The absolute amount adsorbed obtained at 9.89 bar and 303K is 3.7 mol/kg. This value is in coherent with previously reported values (3.34 mol/kg at 318K) at the same pressure [85].

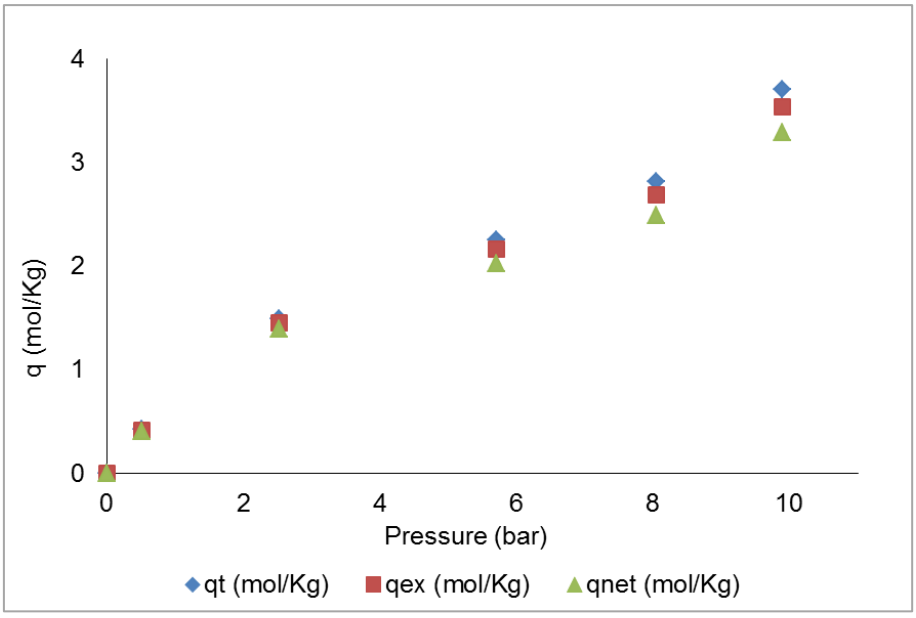

Figure 3.19 - Single-component adsorption equilibrium isotherm for CO_2 at 303K on Fe-BTC.

As for the adsorption isotherm for the Cu-BTC adsorbent the plots also show a classic Langmuir-type isotherm [74] with a well-shaped adsorption curve. Figure 3.20 presents the amount adsorbed in terms of q_{net}, q_{ex} and q_t of CO_2 in Cu-BTC. The absolute amount adsorbed at 5.9 bar (approximately 10.4 mol/Kg) is in agreement with the highest values reported in literature [55][86, 87]. Also the adsorption rapidly increases at pressures below 5 bar and then slowly increases with the increasing pressure. The rate of increase depends on the surface area, at intermediate pressures, and pore volume of the sample at high pressures [88].

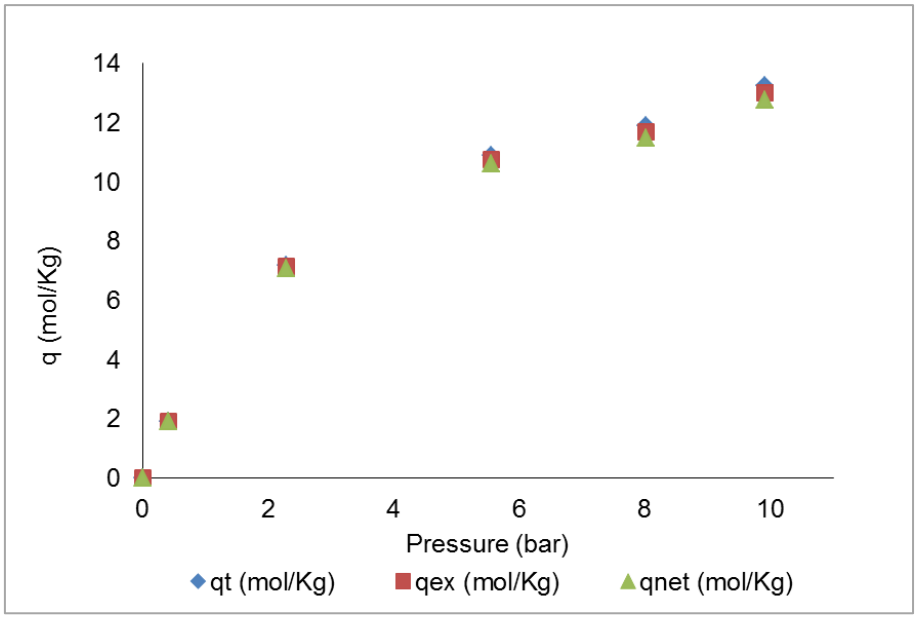

Figure 3.20 - Single-component adsorption equilibrium isotherm for CO_2 at 303K on Cu-BTC.

Cu-BTC show higher adsorption capacity towards CO_2 than Fe-BTC, which can be explained by it larger surface area and pore volume when compared with Fe-BTC. Figures 3.21 and 3.22, presented the comparison of the experimental data obtained in this study for the adsorption equilibrium measurement of CO_2 on Cu-BTC and Fe-BTC, with the data reported in the literature [85] [89], respectively.

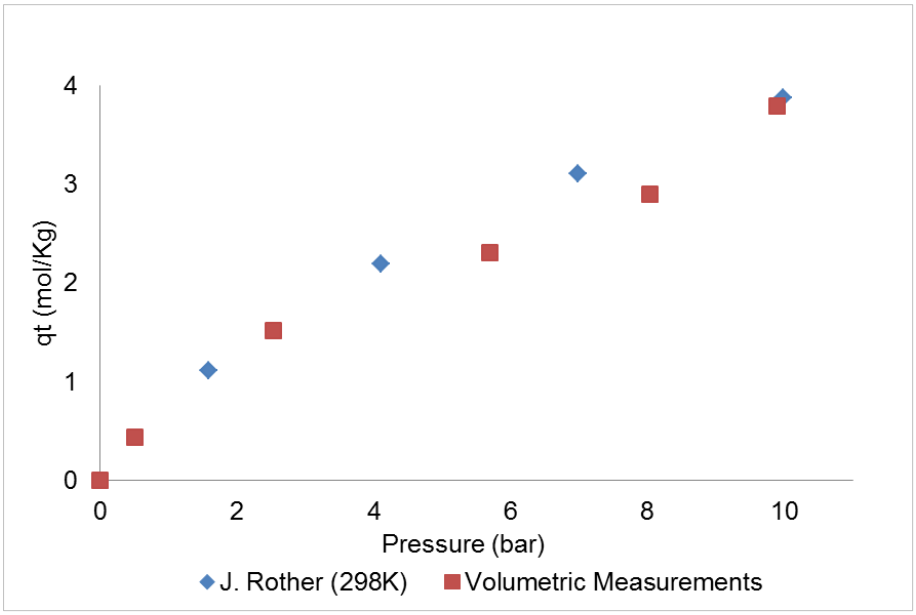

Figure 3.21 – Single-component adsorption equilibrium isotherm of CO_2 at 303K on Fe-BTC. Comparison with the Deniz and co-workers data [85].

It is possible to observe that the measurements are in accordance, even though the temperatures are slightly different. The last point of each isotherm presents a higher adsorption capacity due to the fact that is attributed to experimental difficulties related with the adsorption cell characteristics, as described earlier.

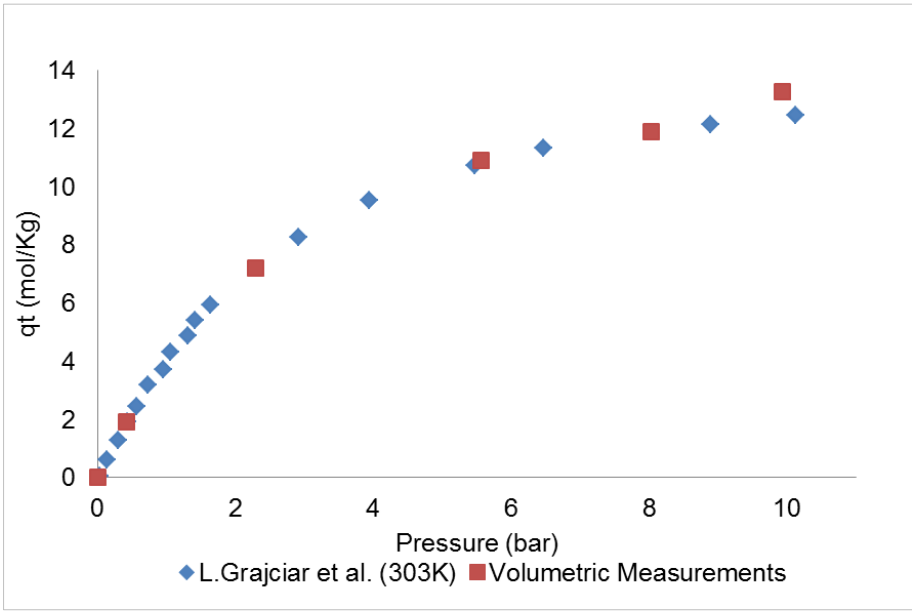

Figure 3.22 - Single-component adsorption equilibrium isotherm of CO_2 at 303K on Cu-BTC- Comparison with the Grajciar and co-workers data [89].

Fe-BTC show the lowest adsorption capacity with a significantly difference in the amount of gas adsorbed compared with Cu-BTC which present a much higher absolute amount adsorbed which is expected due to its higher surface area. This is a very attractive characteristic for gas separation purposes since the adsorbent shows great adsorption capacity.

3.7. Summary

In this chapter, the obtained results for the adsorption equilibrium of ethane in ANG5 and MIL-53(Al) at 303, 323 and 373K were presented. These experimental data presented a big influence of solenoid valves malfunctioning an upgrade to the experimental unit was proposed.

The upgrade of the original unit consisted in the substitution of the solenoid valves for manual ball valves and additionally, the apparatus design was also modified to enable testing a new method for volumetric adsorption equilibrium measurements. The revamped volumetric unit presented different reference volumes compared with the original apparatus reason why the reference and cell volumes had to be recalibrated.

The validation of the upgraded volumetric apparatus was done by measuring the adsorption equilibrium isotherms of CO_2 in ANG6 and ACHM at 323K of temperature and the obtained results were compared with data previously obtained using a high-precision high-pressure gravimetric unit. The experimental results obtained in both apparatuses presented a very good agreement thus validating the operation of the revamped volumetric unit.

Adsorption equilibrium of CO_2 on two different metal organic frameworks: CU-BTC and Fe-BTC at 303K was also measured. The experimental results obtained are in accordance with the experimental data available in the literature. The Cu-BTC presented a higher adsorption capacity when compared to Fe-BTC confirming its interest as an adsorbent for CO_2 separation and storage applications.

4. Alternative Volumetric Method for Adsorption Equilibrium Determination

In this chapter an alternative method for the measurement adsorption equilibria using the upgraded volumetric unit is presented. Unlike the traditional method, in which the temperature is maintained constant and sequential steps of pressure increase and subsequent expansion are performed, in this alternative route a certain amount of adsorbate is fed into the adsorption cell and the temperature in then changed.

The alternative method proposed was evaluated experimentally in the upgraded volumetric unit to measure the adsorption equilibrium of CO_2 on ANG6 and the ACHM at 303, 323, and 353K.

4.1. Experimental Description

The first step of the experimental procedure for this method is similar to the procedure described in Chapter 3. After the activation of the adsorbents, the gas locked in the reference volume (V_{ref}) represented in green in Figure 4.1, is expanded to the sample cells by opening the valves V4, V5, V8 and V9 and adsorption occurs at constant temperature of 303K, controlled by the oven.. Equilibrium is reached after a minimum of 2 hours. This is assumed to occur, when the pressure measurements remain constant for a determined period of time (approximately, one hour).

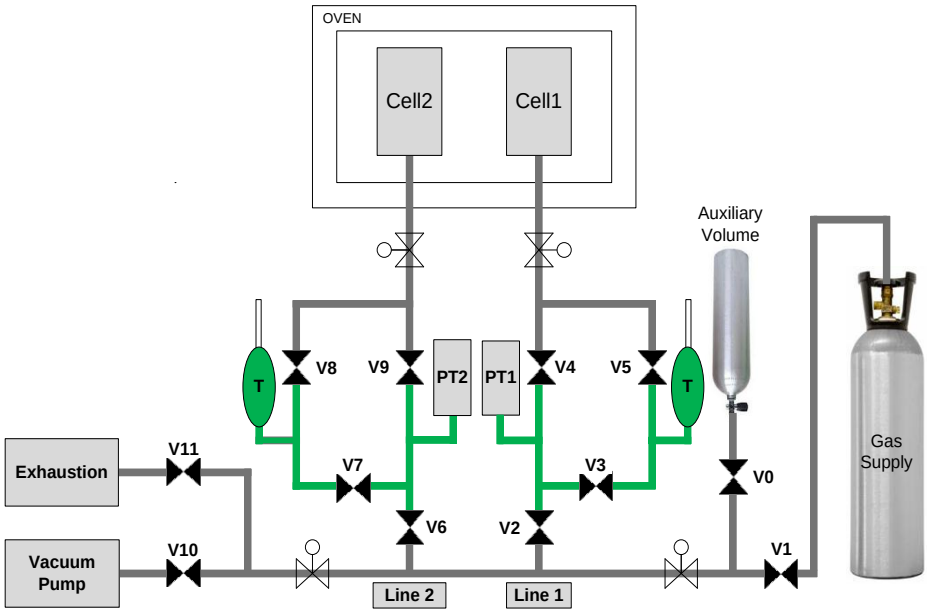

Figure 4.1 - Schematic representation of the first step of measurement in the volumetric unit. Green represents the reference volume (V_{ref}).

After reaching the equilibrium, valves V3, V5, V7 and V8 are closed and the temperature of the oven (containing the adsorption cell) is changed. By using this valve arrangement, the extra volumes which represent almost all the reference volume and are maintained at ambient temperature, can be isolated from the adsorption cell. This way, in substitution of V_{ref}, a much smaller volume (V'_{ref}) is considered as showed in Figure 4.2. The volumes employed in the adsorption equilibrium calculations are showed in Table 4.1.

Table 4.1 – Upgraded volumetric units calibrated

Results	Line 1	Line 2
V_{cell} (cm^3)	2.03 ± 0.01	1.93 ± 0.01
V_{ref} (cm^3)	41.54 ± 0.03	41.51 ± 0.03
V'_{ref} (cm^3)	2.60 ± 0.01	2.56 ± 0.01

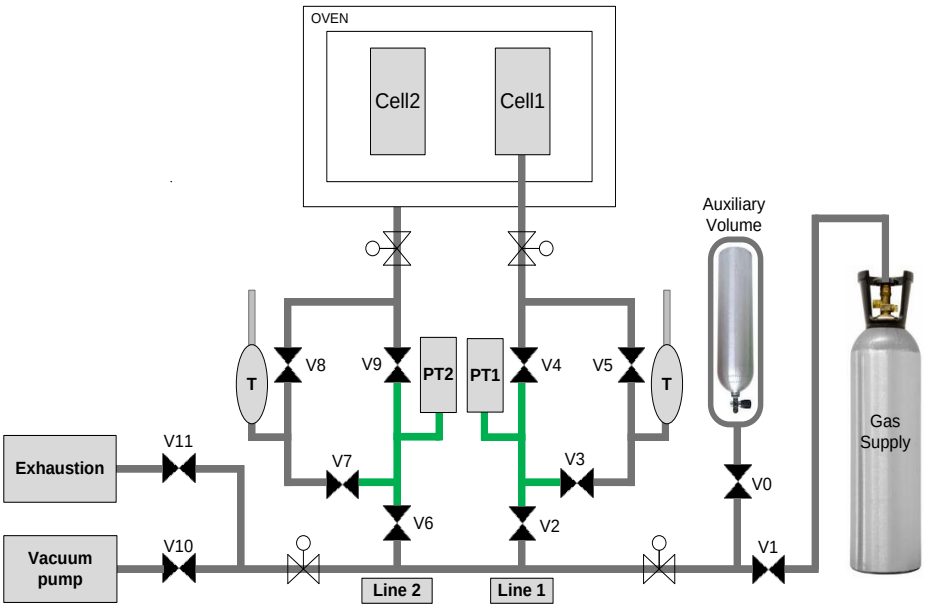

Figure 4.2 - Schematic representation of the second step in the volumetric unit. Green represents the reference volume (V'_{ref}).

The temperature is then raised from 303K to 323K with at a heating rate ok 2K/min. The pressure is registered in the in-house developed software [69] and in Figure 4.3 an example of the pressure change during the temperature raised is showed. The pressure increase, caused by temperature raise in the system is showed. This occurs due to the linear relation between pressure and temperature (equation 5), and also because of the increasing amount of desorbed molecules in the gas phase.

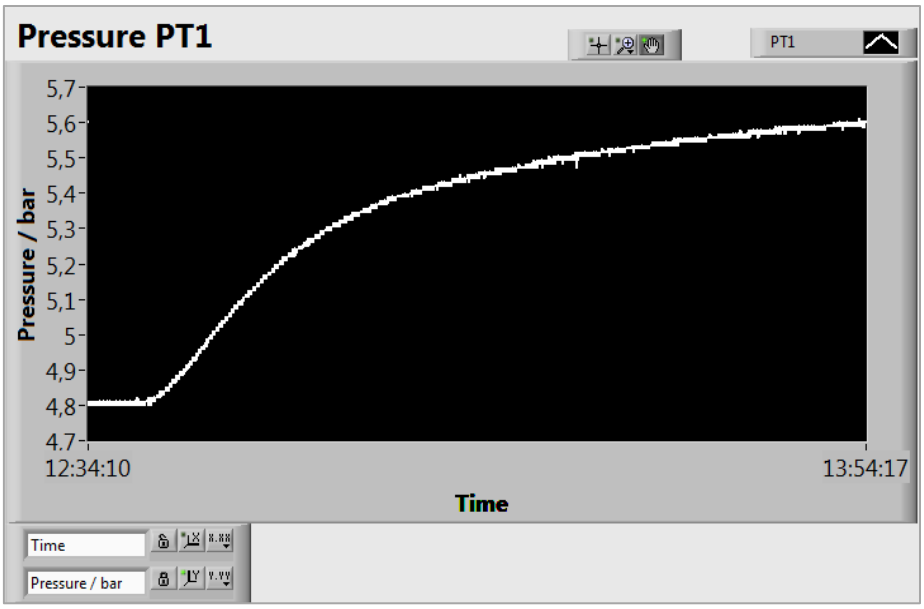

Figure 4.3 – Experimental Pressure History at PT1 during Temperature Raise from 303K to 323K.

After reaching a constant value of pressure for at least one hour, the equilibrium is assumed to be reached and the pressure value recorded is averaged over a period of 10 minutes. Then, the temperature is raised again from 323K to 353K at the same heating rate for approximately 15 minutes. After reaching the equilibrium at 353K, V3, V4, V5, V7, V8 and V9 are opened and the adsorbent sample is cooled to 303K overnight. Then the described procedure is repeated. This method is less time consuming because, unlike the traditional method, the adsorbents are not reactivated between isotherms.

4.2. Experimental Results and Discussion

The adsorption equilibrium of CO_2 on ANG6 and the ACHM, at 303, 323 and 353K obtained using the alternative method described are presented in Figures 4.4 and 4.5. The respective experimental data in terms of absolute amount adsorbed is listed in Appendix H. To determine the adsorption isotherms it should be noted that the measurements at the starting temperature (in this case: 303K) where the gas is expanded, must consider the reference volume (V_{ref}) presented earlier in Figure 4.1 and the following measurements (at 323 and 353K) must use the reference volume (V'_{ref}) presented in Figure 4.2 applying the equation (1) referred in Chapter 3. This equation gives the excess amount adsorbed.

Figure 4.4 present CO_2 adsorption equilibrium at 303, 323 and 353K on ANG6 within 0 - 10 bar. Due to an operation error during the experimental procedure, at approximately 2 bar (green point) only one point (at 303K) was obtained.

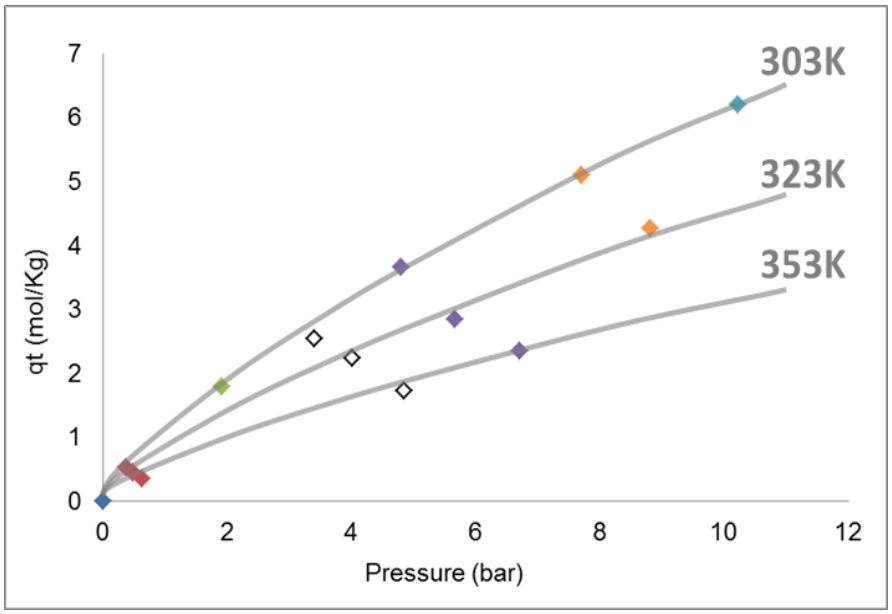

Figure 4.4 – Experimental Single - Component Adsorption Equilibrium of CO_2 on ANG 6 at 303K, 323K and 353K. Each color set represents the results for each constant gas amount fed subjected to the temperature variations. Solid lines are a guide-to-the-eye.

The higher pressure point (light blue) was measured for the three temperatures but with the increase from 303K to 323K the pressure exceeded 10 bar and the previously reported gas leak occurred. For this reason only the 303K data could be obtained at approximately 10 bar.

It is possible to observe that, for both adsorbents, the adsorption capacity decrease with the increasing temperature which is characteristic of the exothermic property of adsorption process. Figure 4.5 presents the adsorption equilibrium of CO_2 at 303, 323 and 353K on ACHM within 0 – 10 bar.

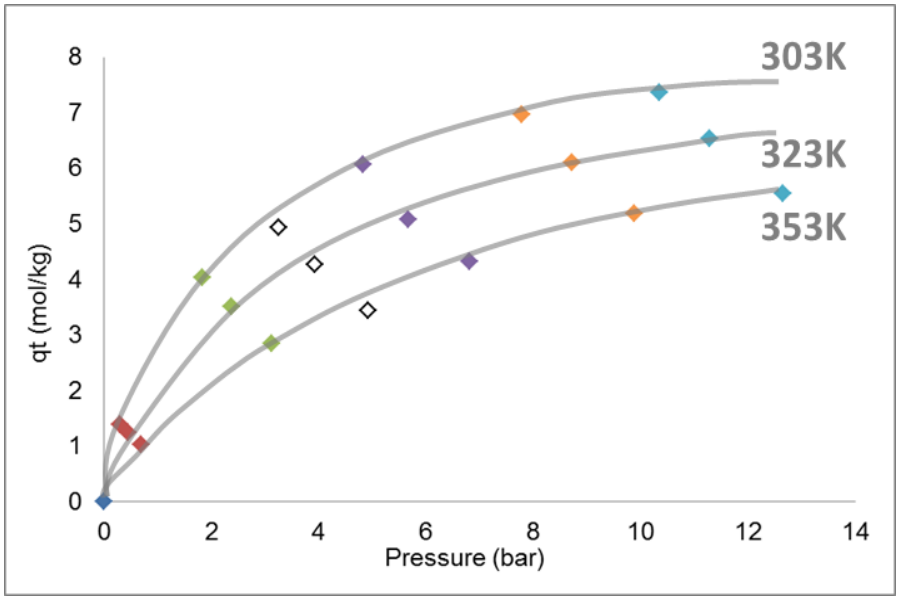

Figure 4.5 - Experimental Single - Component Adsorption of CO2 in ACHM at 303K, 323K and 353K. Each set of color represent the results for a single point of pressure. Solid lines are a guide-to-the-eye.

Figures 4.7 and 4.8 present the comparison between the data obtained using this new method and the data obtained by the research group using the gravimetric method [72]. It is possible to conclude that the adsorption equilibrium of CO_2 on ANG6 and ACHM obtained from the alternative volumetric method and from the gravimetric method are in accordance for the three temperatures studied (view Figures 4.6 and 4.7).

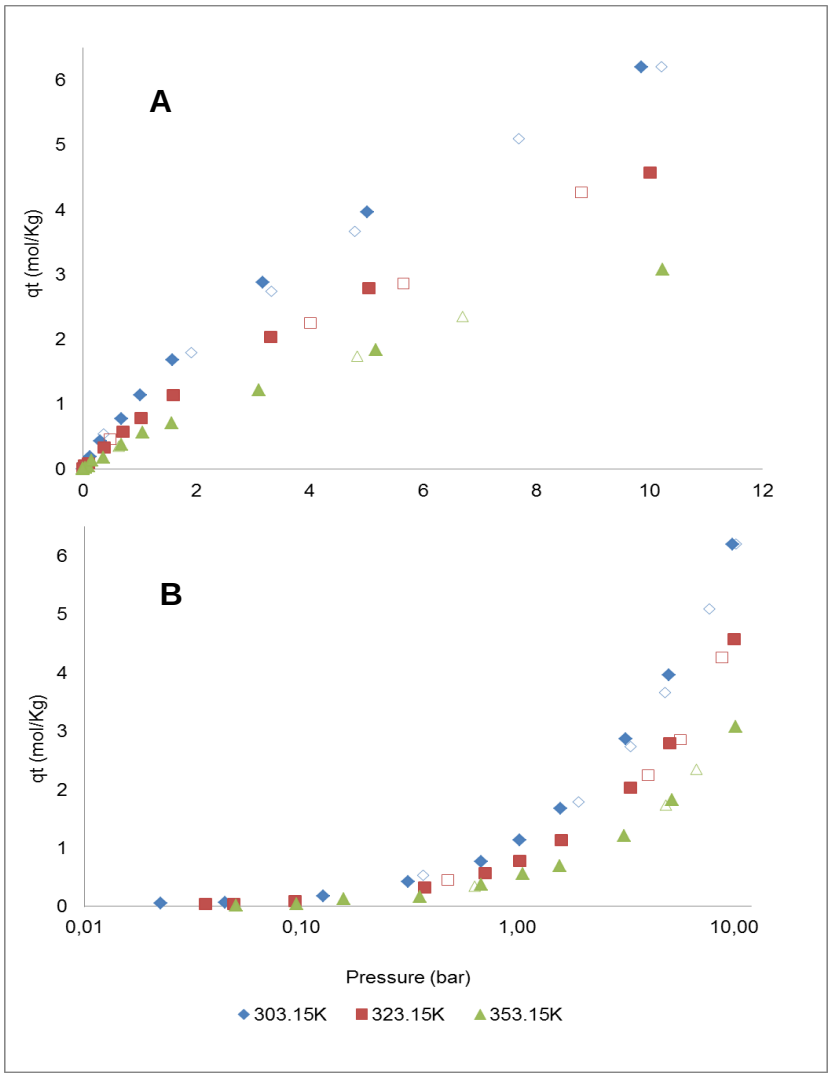

Figure 4.6 – (A) Adsorption isotherms of CO_2 at 303K, 323K and 353K on ANG6. Close symbols denote the gravimetric adsorption data and empty symbols denote the volumetric adsorption data. (B) Represent the experimental results in a logarithm scale.

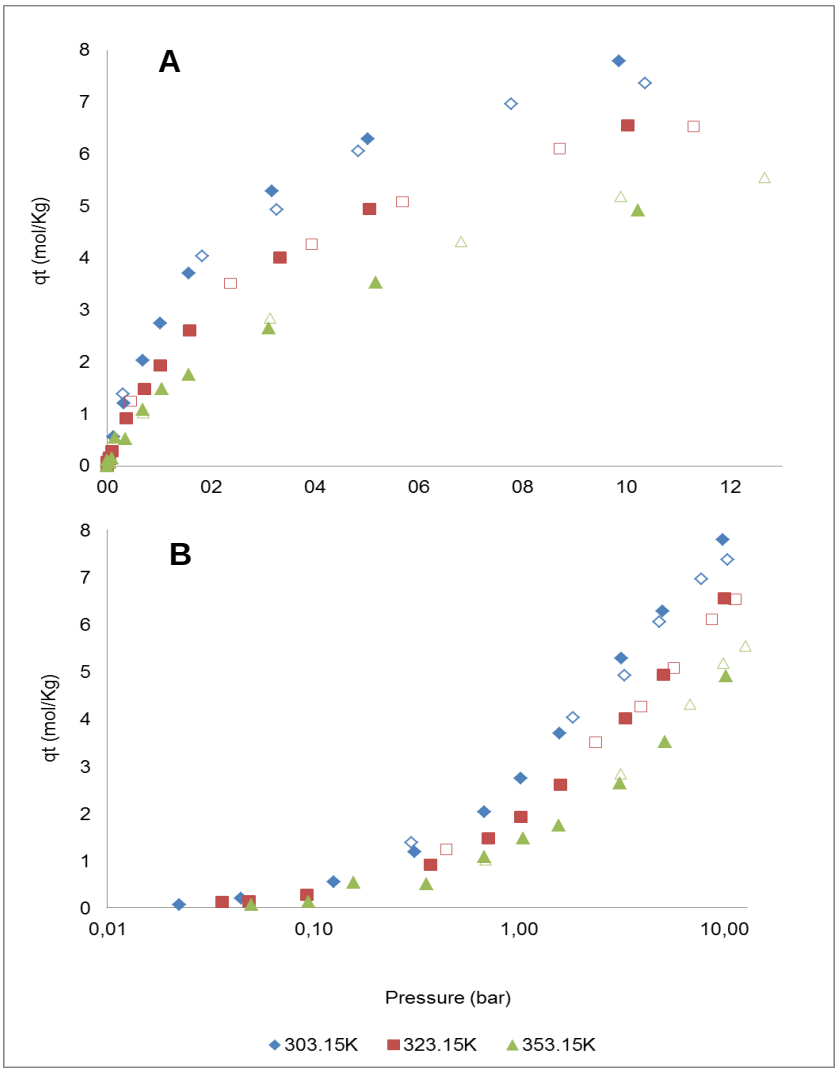

Figure 4.7 - (A) Adsorption isotherms of CO_2 at 303K, 323K and 353K on ACHM. Close symbols denote the gravimetric adsorption data and empty symbols denote the volumetric adsorption data. (B) Represent the experimental results in a logarithm scale.

4.3. Summary

In this chapter, a new method for adsorption equilibrium measurement using volumetric techniques was presented. This method consists in maintaining constant the amount of gas inside the adsorption cell and varying the temperature of the oven containing the adsorption cell. To validate this method, adsorption equilibrium measurements of CO_2 in ANG6 and ACHM were performed at 303, 323, and 353K and compared with experimental data, previously measured using a gravimetric unit. The results showed a satisfactory agreement for the two experimental methods (volumetric and gravimetric) for CO2 adsorption on both adsorbents ensuring that the apparatus is able to perform this method correctly.

This enables the user to determine three adsorption isotherms (or more) by varying the temperature; Also, there is no need for adsorbent re-activation of the samples between isotherms introducing less experimental error.

Chapter V

5. Conclusions and Future Work

A volumetric unit for adsorption equilibrium measurements was tested and upgraded. The solenoid valves existent were substituted for manual ball valves enabling the correct performance of the experimental method. The upgraded laboratorial apparatus is simple, and the operation is straightforward, allowing the measurement of the adsorption equilibria of pure gases over two different adsorbent materials in parallel and at the same time. The revamped volumetric unit can operate between 0 to 20 bar, and over a temperature range of 303 to 1373K.

The validation of the upgraded volumetric operation was made by performing adsorption equilibrium measurements of CO_2 at 323K on ANG6 and ACHM activated carbons. The obtained results were compared with experimental data measured in a gravimetric apparatus, by our group. The good agreement between the results successfully validates the operation of the volumetric unit.

The adsorption equilibrium of CO_2 at 303K on two metal-organic frameworks Cu-BTC and Fe-BTC, was also measured and the results obtained are in accordance with the experimental data available in the literature. These results ensure that the apparatus is operating correctly, the adsorption data is trustable and it can be used to evaluate the adsorption capacity of pure gases over different adsorbents.

A new method to perform the volumetric adsorption equilibrium measurements was also tested and the results are very promising. Adsorption of CO_2 at 303, 323, and 353K on ANG6 and ACHM activated carbons were performed to validate this method. The results were again compared with gravimetrically obtained experimental data. The results obtained in the two different apparatus are in accordance, ensuring that the volumetric unit is able to perform both, the traditional and the alternative methods proposed.

Regarding the future work, improvements have to be done regarding the adsorbent sample. A new adsorption cell must be designed and constructed to ensure that the adsorption equilibrium can be measured between 10 and 20 bar. It would be also interesting to increase the number of lines and adsorption cells of the volumetric unit, enabling the adsorption equilibrium measurements of more than two adsorbents at the same time.

In order to reduce the difference of temperature between the section placed on top of the unit and the sample cells inside the oven, when performing the traditional method for adsorption equilibrium measurements, the temperature of the volumes on top of the volumetric unit should be controlled to reduce the temperature impact when measuring adsorption equilibriums at high temperatures.

Bibliography

[1] Intergovernamental Panel of Climate Change, "Carbon Dioxide Capture and Storage," Cambridge University Press, USA, 2005.

[2] J.-R. Li, Y. Ma, M. C. McCarthy, J. Sculley, J. Yu, H.-K. Jeong, P. B. Balbuena and H.-C. Zhou, "Carbon dioxide capture - related gas adsorption in metal organic frameworks," *Coordination Chemistry Reviews,* vol. 255, pp. 1791-1823, 2011.

[3] NOAA - National Oceanic and Atmospheric Administration, "Earth System Research Laboratory," [Online]. Available: http://www.esrl.noaa.gov/. [Accessed 2 September 2014].

[4] EPA, "Environmental Protection Agency," [Online]. Available: http://www.epa.gov/. [Accessed 2014 September 2014].

[5] N. Hedin, L. Andersson, L. Bergstrom and J. Yan, "Adsorbents for the Post-Combustion Capture of CO2 using Rapid Temperature Swing or Vacuum Swing Adsorption," *Applied Energy,* vol. 104, pp. 418-433, 2013.

[6] A. O. Yazaydin, R. Q. Snurr, T. H. Park, K. Koh, J. Liu, M. D. LeVan, A. I. Benin, P. Jakubczak, M. Lanuza, B. D. Galloway, J. J. Low and R. R. Willis , "Screening of Metal−Organic Frameworks for Carbon Dioxide Capture from Flue Gas Using a Combined Experimental and Modeling Approach," *Journal of American Society,* vol. 131, pp. 18198-18199, 2009.

[7] R. T. Yang, O. R. Davidson, P. R. Bosh, R. Dave and L. A. Meyer, "Contribution of Working Group III to the Fourth Assessment Report of the Intergovernmental Panel on Climate Change," *IPCC,* 2007.

[8] C.-H. Yu, C.-H. Huang and C.-S. Tan, "A Review of CO2 Capture by Absorption and Adsorption," *Aerosol and Air Quality Research,* vol. 12, pp. 745-769, 2012.

[9] S. M. L. Hardie, M. H. Garnett, A. E. Fallick, A. P. Rowland and N. J. Ostle, "Carbon Dioxide Capture Using a Zeolite Molecular Sieve Sampling System for Isotopic Studies (13C and 14C) of Respiration," *Radiocarbon,* vol. 47, pp. 441-451, 2005.

[10] D. Vargas, L. Giraldo and J. Moreno-Piraján, "CO2 Adsorption on Activated Carbon Honeycomb-Monoliths: A comparison of Langmuir and Tóth Models," *International Journal of Molecular Science,* vol. 13, pp. 8388-8397, 2012.

[11] J. Liu, P. Thallaoally, B. P. McGrail , D. Brown and J. Liu, "Progress in adsorptio-based CO2 capture by metal-organic frameworks," *The Royal Society of Chemistry,* vol. 41, pp. 2308-2322, 2012.

[12] R. Yang, Gas Separation by Adsorption Processes, USA: Butterworth Publishers, 1987.

[13] D. M. Ruthven, S. Farroq and K. S. Knaebel, Pressure Swing Adsorption, New York: VCH Publishers, 1994.

[14] F. Rouquerol, J. Rouquerol and K. Sing, Adsorption By Powders & Porous Solids - Principles, Methodology and Applications, França: Academic Press, 1999.

[15] J. Keller and R. Staudt, Gas Adsorption Equilibria - Experimental Methods Adsorption Isotherms, United States of America: Springer, 2005.

[16] D. D. Do, "Adsorption analysis: Equilibria and Kinetics," in *Series on Chemical Engineering*, USA, Emperial College Press.

[17] K. S. Sing, D. H. Everett, R. A. Haul, L. Moscou, R. A. Pieroitti, J. Rouquerol and T. Siemieniewska, "Reporting Physisorption Data for Gas/Solid Systems with Special Reference to the Determination of Surface Area and Porosity," *Pure & App!. Chem.,* vol. 57, pp. 603-619, 1985.

[18] D. M. Ruthven, Principles of Adsorption and Adsorption Processes, Canada: John Wiley & Sons, Inc., 1984.

[19] A. L. Kohl and R. B. Nielsen, "Gas Dehydration and Purification by Adsorption," in *Gas Purification*, Library of Congress Cataloging - in - Publication Data, 1997, pp. 1022 - 1135.

[20] A. Shivaji Sircar, "Separation of Multicomponent Gas Mixtures". US Patent 4,171,206, 21 Aug. 1978.

[21] A. M. Ribeiro, C. A. Grande, F. S. Lopes, J. M. Loureiro and A. E. Rodrigues, "A parametric study of layered bed PSA for hydrogen purification," *Chemical Engineering Science,* vol. 63, pp. 5258-5273, 2008.

[22] A. M. Ribeiro, C. A. Grande, F. V. Lopes, J. M. Loureiro and A. E. Rodrigues, "Four Beds Pressure Swing Adsorption for Hydrogen Purification: Case of Humid Feed and Activated Carbon Beds," *AIChE Journal,* vol. 55, pp. 2292-2302, 2009.

[23] A. D. Ebner and J. A. Ritter, "State-of-the-art Adsorption and Membrane Separation Processes for Carbon Dioxide Production from Carbon Dioxide Emitting Industries,"

Separation Science and Technology, vol. 44, pp. 1273-1421, 2009.

[24] J. Pires, V. K. Saini and M. L. Pinto, "Studies on Selective Adsorption of Biogas Components on Pillared Clays: Approach for Biogas Improvement," *Environmental Science & Technology,* vol. 42, pp. 8727-8732, 2008.

[25] C. A. Grande and A. E. Rodrigues , "Layered Vacuum Pressure-Swing Adsorption for Biogas Upgrading," *American Chemical Society,* vol. 46, pp. 7844-7848, 2007.

[26] R. Wakasugi and A. Kodama, "Dual Reflux PSA Process Applied to VOC Recovery as Liquid Condensate," *Adsorption,* vol. 11, pp. 561-566, 2005.

[27] R. C. Bansal and M. Goyal, Activated Carbon Adsorption, CRC Press - Taylor and Francis Group, 2005.

[28] A. Dabrowski, "Adsorption - from theory to practice," *Advances in Colloid and Interface Science ,* vol. 93, pp. 135-224, 2001.

[29] A. Khalid, *Experimental Investigation and Mathematical Modeling of a Low Energy Consuming Hybrid Desiccant Cooling System for Hot and Humid Areas of Pakistan,* Pakitan Rsearch Repository, 2008, pp. 36 - 47.

[30] R. T. Yang, Adsorbents: Fundamentals and Applications, Canada: Wiley-Interscience, 2003.

[31] I. A. A. C. C. Esteves, M. S. S. Lopes, P. M. C. Nunes and J. P. B. Mota, "Adsorption of natural gas and biogas components on activated carbon," *Separation and Purification Tecnology,* vol. 62, pp. 281-296, 2008.

[32] W. Olds and Y. Xue, "Remediation of PAH Contaminated Soils and Groundwater using Activated Carbon," ENNR 429: Midyear Report, 2009.

[33] Chemviron Carbon, "Activated Carbon as a Catalyst or for Catalyst Support," 2014. [Online]. Available: http://www.chemvironcarbon.com/. [Accessed 3 September 2014].

[34] D. Lozano-Castello, J. Alcaniz-Monge, M. A. Casa-Lillo, D. Cazorla-Amorós and A. Linares-Solano, "Advances in the study of methane storage in porous carbonaceous materials," *Fuel,* vol. 81, pp. 1777-1803, 2002.

[35] W. Olds and Y. Xue, "Remediation of PAH Contaminated Soils and Groundwater using," *Milyear Report,* vol. ENNR 429, 2009.

[36] F. Rezaei and P. Webley, "Structured Adsorbents in Gas Separation Processes,"

Separation and Purification Technology, vol. 70, pp. 243-256, 2010.

[37] S. Wallace and L. Hench, "Structural Analysis of Water in Silica Gel," *Journal of Sol-Gel Science and Technology,* vol. 1, pp. 153-168, 1994.

[38] H. Chua, A. Chakraborty, N. Oo and M. Othman, "Adsorption Characteristics of Silica Gel + Water Systems," *Journal of Chemical Engineering Data,* vol. 47, pp. 1177-1181, 2002.

[39] F. Bartell and J. Bower, *Adsorption of Vapours by Silica Gels of Different Structures,* University of Michigan, 1951.

[40] S. Ma and H.-C. Zhou, "Gas storage in porous metal-organic frameworks for clean energy applications," *The Royal Society of Chemistry,* vol. 46, pp. 44-53, 2010.

[41] M. E. Davis, "Ordered porous materials for emerging applications," *Nature,* vol. 417, pp. 813-821, 2002.

[42] Y. Yan, M. Suyetin, E. Bichoutskaia, A. J. Blake, D. R. Allan, S. A. Barnett and M. Schröder, "Modulating The packing of [Cu24(isophthalate)24] cuboctahedra in triazole-containing metal-organic polyhedral framework," *The Royal Society of Chemistry,* vol. 4, pp. 1731-1736, 2013.

[43] J.-R. Li, R. J. Kuppler and H.-C. Zhou, "Selective gas adsorption and separation in metal–organic frameworks," *Chemical Society Reviews,* vol. 38, pp. 1477-1504, 2009.

[44] H. Furukawa, K. E. Cordova, M. O'Keeffe and O. M. Yaghi, "The Chemistry and Applications of Metal-Organic Frameworks," *Science,* vol. 341, p. 974, 2013.

[45] A. Lyubchyk, I. A. A. C. Esteves, F. J. A. L. Cruz and J. P. B. Mota, "Experimental and Theoretical Studies of Supercritical Methane Adsorption in the MIL-53(Al) Metal Organic Framework," *The Journal of Physical Chemistry,* vol. 115, pp. 20628-20638, 2011.

[46] N. A. Ramsalhye, G. Maurin, S. Bourrelly, P. L. Llewellyn, C. Serre, T. Loiseau, T. Devic and G. Férey, "Probing the Adsorption Sites for CO2 in Metal Organic Frameworks Materials MIL-53 (Al, Cr) and MIL-47 (V) by Density Functional Theory," *American Chemical Society,* vol. 112, pp. 514-520, 2008.

[47] A. Boutin, F. Coudert, A. Springuel-Huet, A. V. Neimark, G. Férey and A. H. Fuchs, "The Behavior of Flexible MIL-53(Al) upon CH4 and CO2 Adsorption," *Journal of Physical Chemistry,* vol. 114, pp. 22237-22244, 2010.

[48] J. M. Catillo, T. J. H. Vlugt and S. Calero, "Understanding Water Adsorption in Cu-BTC Metal-Organic Frameworks," *American Chemical Society,* vol. 112, no. 41, pp. 15934-

15939, 2008.

[49] BASF, Chemical Company;, "Basolite Metal Organic Frameworks," [Online]. Available: http://www.sigma-aldrich.com. [Accessed 17 June 2014].

[50] Y. Yang , P. Shukla, S. Wang, V. Rudolph, X.-M. Chen and Z. Zhu, "Significant improvement of surface area and CO2 adsorption of Cu–BTCviasolvent exchange activation," *The Royal Society of Chemistry,* vol. 3, pp. 17065-17072, 2013.

[51] J. J. Gutiérrez-Sevillano, J. M. Vicent-Luna, D. Dubbeldam and S. Calero, "Molecular Mechanisms for Adsorption in Cu-BTC Metal Organic Framework," *The Journal of Physical Chamistry,* vol. 117, pp. 11357-11366, 2013.

[52] C. Prestipino, L. Regli, J. G. Vitillo, F. Bonino, A. Damin, C. Lamberti, A. Zecchina, P. L. Solari, K. O. Kongshaung and S. Bordiga, "Local Structure of Framework Cu(II) in HKUST-1 Metallorganic Framework: Spectroscopic Characterization upon Activation and Interaction with Adsorbates," *American Chemica Society,* vol. 18, pp. 1337-1346, 2006.

[53] S. Cavenati, C. A. Grande, A. E. Rodrigues, C. Kiener and U. Muller, "Metal Organic Frameworks Adsorbents for Biogas Upgrading," *Industrial & Engineering Chemist Research,* vol. 47, pp. 6333-6335, 2008.

[54] L. Wu, J. Xiao, Y. Wu, S. Xian, G. Miao, H. Wang and Z. Li, "A Combined Experimental/Computational Study on the Adsorption of Organosulfur Compounds over Metal−Organic Frameworks from Fuels," *Langmuir,* vol. 30, pp. 1080-1088, 2014.

[55] Z. Liang, M. Marshal and A. L. Chaffee, "CO2 Adsorption-Based Separation by Metal Organic Framework (Cu-BTC) versus Zeolite (13X)," *Energy & Fuels,* vol. 23, pp. 2785-2789, 2009.

[56] "H2 and CH4 Sorption on Cu-BTC Metal Organic Frameworks at Pressures up to 15 MPa and Temperatures between 273 and 318 K," *Journal of Surface Engineered Materials and Advanced Technology,* vol. 1, pp. 23-29, 2011.

[57] J. Rother, T. Feiback, R. Seif and F. Dreisbach, "Characterization of solid and liquid sorbent materials for biogas purification by using a new volumetric screening instrument," *Review of Scientific Instruments,* vol. 83, 2012.

[58] "An Experimental Study of Adsorption Breakthrough Curves for CO2/CH4 Separation in a Fixed Bed of Nanoporous Shaped Copper Trimesate Metal Organic Framework," *Iranian Journal of Oil & Gas Science and Technology,* vol. 2, pp. 54-66, 2013.

[59] G. Majano, O. Ingold, M. Yulikov, G. Jeschke and J. Pérez-Ramírez, "Room-temperature

synthesis of Fe-BTC from layered iron hydroxides: the influence of the percursor organization," *The Royal Society of Chemistry,* vol. 15, pp. 9885-9892, 2013.

[60] A. Micek-Ilnicka and B. Gil, "Heteropolyacid encapsulation into MOF: Influence of acid particles distribution on ethanol conversation in hybrid nanomaterials," *The Royal Society of Chemistry,* vol. 41, pp. 12624-12629, 2012.

[61] A. Dhakshinamoorthy, M. Alvaro and H. Garcia, "Atmospheric-Pressure, Liquid-Phase, Selective Aerobic Oxidation of Alkanes Catalysed by Metal–Organic Frameworks," *Chemistry European Journal,* vol. 17, pp. 6256-6262, 2011.

[62] P. L. Llewellyn, S. Bourrelly, C. Serre, A. Vimont, M. Daturi, L. Hamon, G. Weireld, J.-S. Chang, D. Hong, Y. Hwang, S. Jhung and G. Férey, "High Uptakes of CO2and CH4in Mesoporous MetalsOrganic Frameworks MIL-100 and MIL-101," *Langmuir,* vol. 24, pp. 7245-7250, 2008.

[63] M. Latroche , S. Surblé, C. Serre, C. Mellot-Draznieks, P. Llewellyn , J.-H. Lee, J.-S. Chang , S. H. Jhung and G. Férey, "Hydrogen Storage in the Giant-Pore Metal–Organic Frameworks MIL-100 and MIL-101," *Angewandte Chemie,* vol. 45, pp. 8227-8231, 2006.

[64] F. Jaremias, A. Khutia, S. Henninger and C. Janiak, "MIL-100(Al, Fe) as water adsorbents for heat transformation purposes - a promising application," *Journal of Materials Chemistry,* vol. 22, pp. 10148-10151, 2012.

[65] J. B. Condon, Surface Area and Porosity Determinations by Physisorption, Amsterdam: Elsevier, 2006.

[66] Y. Belmabkhout, M. Frère and G. D. Weireld, "High-pressure adsorption measurements. A comparative study of the volumetric and gravimetric methods," *Measurements Science and Technology,* vol. 15, pp. 848-858, 2004.

[67] O. Talu and A. L. Myers, "Molecular Simulation of Adsorption: Gibbs Dividing Surface and comparison with Experiment," *AIChE Journal,* vol. 47, pp. 1160-1168, 2001.

[68] J. B. Condon, Surface Area and Porosity Determinations by Physisorption Mesurements and Theory, USA: ELSEVIER, 2006.

[69] J. S. Correia Gomes, "Experimental High-Throughput Adsorption Unit for Multi-Evaluation of Adsorbents for Gas Capture, Storage and Separation Applications," MSc. Thesis, Faculdade de Ciencias e Tecnologia - Universidade Nova de Lisboa, 2014.

[70] I. A. Esteves, "Gas Separation Processes By Integrated Adsorption And Permeation Technologies," Phd Thesis, Faculdade de Ciências e Tecnologia, Universidade Nova de

Lisboa, 2005.

[71] B. Camacho, "Experimental Gravimetric Adsorption Equilibrium of n-Alkanes and Alkenes, Carbon Dioxide and Nitrogen in MIL-53(Al) and Zeolite 5A," MSc. Thesis, Faculdade de Ciencias e Tecnologia - Universidade Nova de Lisboa, 2014.

[72] I. Valente, "Adsorption equilibria of flue gas components on activated carbon," MSc. Thesis, Faculdade de Ciência e Tecnologia, Universidade Nova de Lisboa, 2014.

[73] A. Lyubchyk, "Gas Separation in the Mil-53(Al) Metal Organic Framework. Experiments and Molecular Simulation," Phd. Thesis, Faculdade de Ciências e Tecnologia, Universidade Nova de Lisboa, 2013.

[74] S. Lowell, Characterization of Porous Solids and Powders: Surface Area, Pore Size and Density, Springer Science & Business Media, 2004.

[75] K. Sing, D. Everett, R. Haul, L. Moscou, R. Pierotti, J. Rouquérol and T. Siemieniewska, "Reporting Physisorption Data for Gas/Solid Systems," *Pure and Applied Chemistry,* vol. 57, no. 4, pp. 603-619, 1985.

[76] R. P. P. L. Ribeiro, R. J. S. Silva, I. A. A. C. Esteves and J. P. B. Mota, "A Multi-Sample Volumetric Apparatus for Chamical Education: A study of Gas Adsorption Equilibrium," *Journal of Chemical Education,* 2014.

[77] S. Bourrelly, P. Llewellyn, C. Serre, F. Millange, T. Loiseau and G. Férey, "Different Adsorption Behaviors of Methane and Carbon Dioxide in the Isotypic Nanoporous Metal Terephthalates MIL-53 and MIL-47," *J. AM. CHEM. SOC. ,* vol. 127, pp. 13519-13521, 2005.

[78] NIST, "National Institute of Standards and Technology," 2011. [Online]. Available: http://webbook.nist.gov/. [Accessed 04 August 2014].

[79] S. Gumma and O. Talu, "Net adsorption: A thermodynamic Framework for Supercritical Gas Adsorption and Storage in Porous Solids," *Langmuir,* vol. 26, pp. 17013-17023, 2010.

[80] Instituto Português do Mar e Atmosfera, "impa," [Online]. Available: http://www.ipma.pt/. [Accessed 5 June 2014].

[81] A. Badalyan and P. Pendleton, "Analysis of Uncertanties in Manometric Gas-Adsorption Measurements," *Langmuir,* vol. 19, pp. 7919-7928, 2003.

[82] LCGM, "Evaluation of measurement data - Guide to the expression of uncertainty in

measurement," *GUM,* vol. 100, pp. 8-24, 2008.

[83] T. Van Assche, . T. Remy, G. Desmet, G. Baron and J. Denayer, "Adsorptive separation of liquid water/acetonitrile mixtures," *Separation and Purification Technology,* vol. 82, pp. 76-86, 2011.

[84] J. Ploegmakers, S. Japip and K. Nijmeijer, "Mixed matrix membranes containing MOFs for ethylene/ethane separation. Part A: Membrane preparation and characterization," *Journal of Membrane Science,* vol. 428, pp. 445-453, 2013.

[85] E. Deniz, F. Karadas, S. Aparicio, C. T. Yavuz, . H. A. Patel and M. Atilhan, "A combined computational and experimental study of high pressure and supercritical CO2 adsorption on Basolite MOFs," *Microporous and Mesoporous Materials,* vol. 175, pp. 34-42, 2013.

[86] J. R. Karra and K. S. Walton, "Molecular Simulations and Experimental Studies of CO2, CO, and N2 Adsorption in Metal-Organic Frameworks," *Journal of Physical Chemestry,* vol. 114, pp. 15735-15740, 2010.

[87] P. Chowdhury, . C. Bikkina, D. Meister, F. Dreisbach and . S. Gumma, "Comparison of adsorption isotherms on Cu-BTC metal organic frameworks synthesized from different routes," *Microporous and Mesoporous Materials ,* vol. 117, pp. 406-413, 2009.

[88] H. Frost, T. Düren and R. Q. Snurr, "Effects of Surface Area, Free Volume, and Heat of Adsorption on Hydrogen Uptake in Metal-Organic Frameworks," *Journal of Physical Chemistry,* vol. 110, pp. 9565-9570, 2006.

[89] L. Grajciar, A. D. Wiersum, P. L. Llewellyn, J.-S. Chang and P. Nachtigall, "Understanding CO2Adsorption in CuBTC MOF: Comparing Combined DFT-ab Initio Calculations with Microcalorimetry Experiments," *Journal of Physical Chemistry,* vol. 115, pp. 17925-17933, 2011.

[90] P. Kusgens, A. Zgaverdea, S. Siegle, H. G. Fritz and S. Kaskel, "Metal-Organic Frameworks in Monolithic Structures," *Journal of the American Ceramic Saociety,* vol. 93, pp. 2476-2479, 2010.

Appendix

Appendix A – Experimental ethane (C_2H_6) adsorption equilibrium data on the carbon sample ANGUARD5 at 303, 323 and 373K. Seven experimental points were measured.

ANG5					
303K		**323K**		**373K**	
Pressure (bar)	qt (mol/Kg)	Pressure (bar)	qt (mol/Kg)	Pressure (bar)	qt (mol/Kg)
0,00	0,00	0,00	0,00	0,00	0,00
0,81	2,59	0,53	1,50	1,12	1,26
3,66	4,99	2,08	3,24	3,83	2,62
6,39	7,24	4,22	4,51	6,58	3,48
11,52	8,13	7,44	5,71	10,69	4,50
		11,33	6,78	14,07	5,70
		15,65	7,29	17,07	6,41

Appendix B – Experimental ethane (C_2H_6) adsorption equilibrium data on the MOF sample MIL-53 (Al) at 303, 323 and 373K. Seven experimental points were measured.

MIL-53 (AL)					
303K		**323K**		**373K**	
Pressure (bar)	qt (mol/Kg)	Pressure (bar)	qt (mol/Kg)	Pressure (bar)	qt (mol/Kg)
0,00	0,00	0,00	0,00	0,00	0,00
0,78	2,17	0,47	1,34	1,05	1,23
3,82	2,95	2,13	2,36	3,84	2,10
6,73	4,00	4,30	2,94	6,61	2,42
11,37	3,87	7,51	3,38	10,75	2,86
		11,41	3,76	14,11	3,63
		15,72	3,82	17,18	4,02

Appendix C – Experimental carbon dioxide (CO_2) adsorption equilibrium data on the carbon sample ANGUARD6 at 323K. Nine experimental points were measured.

ANG6			
Pressure (bar)	**qnet (mol/kg)**	**qex (mol/kg)**	**qt (mol/Kg)**
0,00	0,00	0,00	0,00
0,21	0,25	0,25	0,26
0,61	0,55	0,56	0,58
1,11	0,86	0,88	0,92
1,99	1,34	1,37	1,44
3,47	1,96	2,01	2,14
5,29	2,90	2,97	3,17
8,21	3,98	4,10	4,41
10,28	4,69	4,84	5,23

Appendix D – Experimental carbon dioxide (CO_2) adsorption equilibrium data on the carbon sample ACHM honeycomb monolith at 323K. Nine experimental points were measured.

ACHM			
Pressure (bar)	**qnet (mol/kg)**	**qex (mol/kg)**	**qt (mol/Kg)**
0,00	0,00	0,00	0,00
0,18	0,71	0,71	0,72
0,57	1,55	1,56	1,58
1,08	2,41	2,42	2,46
1,97	3,32	3,35	3,42
3,46	4,40	4,44	4,57
5,32	5,20	5,27	5,47
8,27	6,04	6,15	6,47
10,35	6,20	6,34	6,73

Appendix E – Experimental carbon dioxide (CO_2) adsorption equilibrium data on the MOF sample Fe-BTC at 303K. Seven points were measured

Fe-BTC			
Pressure (bar)	**qnet (mol/kg)**	**qex (mol/kg)**	**qt (mol/kg)**
0,00	0,00	0,00	0,00
0,51	0,40	0,42	0,42
2,52	1,39	1,45	1,49
5,70	2,03	2,16	2,26
8,04	2,49	2,69	2,82
9,89	3,29	3,54	3,70
12,72	4,72	5,04	5,25

Appendix F – Experimental carbon dioxide (CO_2) adsorption equilibrium data on the MOF sample Cu-BTC at 303K.

Cu-BTC			
Pressure (bar)	**qnet (mol/kg)**	**qex (mol/kg)**	**qt (mol/kg)**
0,00	0,00	0,00	0,00
0,42	1,89	1,90	1,91
2,28	7,08	7,13	7,19
5,55	10,62	10,75	10,89
8,02	11,47	11,67	11,87
9,92	12,74	12,99	13,24
12,79	13,59	13,92	14,25

Appendix H – Experimental carbon dioxide (CO_2) adsorption equilibrium data on two carbon samples ANG6 and ACHM honeycomb monolith at 303, 323 and 353K. Nine experimental points were measured.

	ANG6		ACHM	
Temperature (K)	**Pressure (bar)**	**qt (mol/kg)**	**Pressure (bar)**	**qt (mol/kg)**
303	0,00	0,00	0,00	0,00
303	0,37	0,54	0,30	1,39
323	0,48	0,45	0,45	1,25
353	0,63	0,35	0,69	1,03
303	1,91	1,79	1,83	4,03
323		2,40	2,37	3,51
353		2,40	3,13	2,85
303	4,80	3,66	4,84	6,06
323	5,66	2,86	5,68	5,08
353	6,70	2,35	6,82	4,32
303	7,70	5,09	7,79	6,97
323	8,80	4,26	8,72	6,11
353		7,09	9,89	5,19
303	3,40	2,55	10,36	7,37
323	4,02	2,25	11,30	6,54
353	4,84	1,74	12,66	5,55
303	10,22	6,21	3,27	4,93
323			3,94	4,26
353			4,93	3,43